


5-2022

Reconstructing Bison and Mammoth Migration During the Late Pleistocene and Early Holocene of Central Texas Using Strontium Isotopes

Joshua John Porter
University of Arkansas, Fayetteville

Follow this and additional works at: <https://scholarworks.uark.edu/etd>

 Part of the [Archaeological Anthropology Commons](#), [Biological and Physical Anthropology Commons](#), [Natural Resources and Conservation Commons](#), and the [Terrestrial and Aquatic Ecology Commons](#)

Citation

Porter, J. J. (2022). Reconstructing Bison and Mammoth Migration During the Late Pleistocene and Early Holocene of Central Texas Using Strontium Isotopes. *Graduate Theses and Dissertations* Retrieved from <https://scholarworks.uark.edu/etd/4451>

This Thesis is brought to you for free and open access by ScholarWorks@UARK. It has been accepted for inclusion in Graduate Theses and Dissertations by an authorized administrator of ScholarWorks@UARK. For more information, please contact uarepos@uark.edu.

Reconstructing Bison and Mammoth Migration During the Late Pleistocene and Early Holocene
of Central Texas Using Strontium Isotopes

A thesis submitted in partial fulfillment
of the requirements for the degree of
Master of Arts in Anthropology

by

Joshua Porter
George Washington University
Bachelor of Science in Biological Anthropology, 2020

May 2022
University of Arkansas

This thesis is approved for recommendation to the Graduate Council.

Amelia Villaseñor, Ph.D.
Thesis Director

John Samuelsen, Ph.D.
Committee Member

Celina Suarez, Ph.D.
Committee Member

Peter Ungar, Ph.D.
Committee Member

Abstract

During the Late Pleistocene (LP; past 130,000 years), over two-thirds of large mammal (>45kg) species went extinct globally. While the role of humans is hotly debated, the effect of these extinctions is growing clearer; the extinctions resulted in widespread and lasting faunal community reorganization. However, the impact of these extinctions on dietary and migratory behavior within faunal communities is unknown. Our study examines the impact of the megafaunal extinctions on the dietary and migratory behavior of surviving Bison individuals in Texas using carbon, oxygen, and strontium isotopes. Strontium isotopes are incorporated into mammalian enamel during their tooth development and varies as these organisms travel to areas with new bedrock. To capture movement within an individual in the fossil record, serially sampling a single tooth can reveal the movements of an individual across space. Here, we examine the carbon, oxygen, and strontium isotopes from the enamel of two ubiquitous Pleistocene genera (Bison and Mammuthus) before the megafaunal extinctions. We preferentially sampled sites older than the commonly cited (12 Ka) date for widespread human occupation in North America. We also sampled Bison that survived the megafaunal extinction to compare migratory patterns before and after the extinction. This study thus presents high-resolution, serially sampled stable isotope data on bison (n=10) and mammoths (n=5) collected from five LP sites, dating from 33 to 11 Ka, in central Texas. Preliminary strontium isotope data suggest that Mammuthus has larger home ranges in Texas (>100km) than modern savannah elephants (30–50km). Our data will reveal important information about the effects of megafaunal extinction on migratory patterns through time. Given the small samples sizes of this study, additional research is needed to refine our understanding of the mechanisms causing this spatial and temporal variation and its relevance to other taxa.

Acknowledgements

I would like to acknowledge the financial support of the National Science Foundation via the Graduate Research Fellowship Program as well as the University of Arkansas Profession Student Congress through their research grant. Research support was provided by the University of Arkansas Stable Isotope Lab and by John Samuelsen on behalf of the Arkansas Archaeological Survey. I would also like to thank the critical support of the Adriana Potra's Radiogenic Isotope Lab and the Erik Pollock's Trace Element and Radiogenic Isotope Lab. Thank you also to the University of Arkansas Villaseñor-Delezene lab for providing feedback on previous presentations of this research. Finally, I am immensely grateful to every member of my committee for their continued support and understanding throughout this process. None of this would have been possible without their involvement.

Dedication

I dedicate this thesis to every generation of Porters and Paters past, present, and future. As a first-generation college graduate, I recognize this thesis as the culmination of over 100 years of struggle and strife for Porters and Paters. 2022 is 143rd anniversary of Jan Pater and the 135th anniversary of Janna Jolman immigrating to the United States from the Netherlands. They risked everything to come to this country for better opportunities for their descendants. I am forever grateful not only to my 3rd great grandparents, but every generation between them and myself for their sacrifices and support to reach this goal.

Table of Contents

1. Introduction	1
1.1. Keystone species and ecosystem engineers	1
1.2. Ecological drivers of migration	2
1.3. Strontium isotopes	4
1.4. Research questions and hypotheses	4
2. Materials and Methods	6
2.1. Materials	6
2.2. Methods	7
2.2.1. Normalized Difference Vegetation Index (NDVI)	7
2.2.2. Enamel sampling	8
2.2.3. Sample preparation and trace element analysis	9
2.2.4. Column chemistry	9
2.2.5. Strontium isotope ratio analysis	10
2.2.6. Geospatial modeling in ArcGIS Pro	10
2.2.7. Two-member mixing models	11
3. Results	12
3.1. Strontium isoscape	12
3.2. Pleistocene mammoth migration	12
3.3. Pleistocene bison migration	14
3.4. Holocene bison migration	16
4. Discussion	17
4.1. Paleoclimate of central Texas during the Late Pleistocene and early Holocene	17
4.2. Pleistocene migration corridors	18
4.3. Holocene migration corridors	20
4.4. Landscape of fear: human impacts on post-extinction communities	21
5. Conclusion	22
6. References	23
7. Figures and Tables	32

List of Figures

Figure 1: Animated NDVI of Texas	32
Figure 2: Isoscape of central Texas with plotted pointed data	33
Figure 3: Site map and Texas major rivers	34
Figure 4: Isoscape of central Texas	35
Figure 5: Strontium ratios of Pleistocene mammoths	36
Figure 6: Strontium ratios of Pleistocene bison	37
Figure 7: Strontium ratios of Holocene bison	38
Figure 8: Strontium ratios of mammoths and bison at Friesenhahn Cave	39
Figure 9: Strontium ratios of mammoths and bison at WMNM	40

List of Tables

Table 1: Site ages and sample sizes	41
Table 2: Mixing models of Pleistocene mammoths	42
Table 3: Mixing models of Pleistocene bison	45
Table 4: Mixing models of Holocene bison	48

1. Introduction

Large mammals face a looming biodiversity crisis that is the direct result of human impacts, such as landscape fragmentation and human hunting. However, this issue is not only confined to the present; during the Late Pleistocene (LP; past 130,000 years) to the Holocene (past 11,700 years), over two-thirds of megafaunal species (taxa weighing ≥ 44 kg) went extinct. In North America, at least 34 genera went extinct (Koch and Barnosky, 2006). While the causes of megafaunal extinctions (e.g. overkill, hyperdisease, climate, etc.) remain contentious, current evidence suggests that climate and humans could have both been major contributing factors (Broughton and Weitzel, 2018). Additionally, the evidence shows that the causal agents of the extinctions vary by region, including in Australia, Africa, Europe, and North America (Koch and Barnosky, 2006). This body size downgrading of mammals over the last 130ka has had cascading, macroecological effects on ecosystems globally, while the local to regional-scale consequences of megafaunal extinction have yet to be revealed (Smith et al., 2019). Here, I explore how large mammal movement patterns changed before and after the megafaunal extinction in central Texas to elucidate regional-scale consequences of megafaunal extinction.

1.1. Keystone species and ecosystem engineers

Ecosystem engineers are organisms that alter resource availability and thus, “modify, maintain and/or create habitats” (Jones et al., 1994). A keystone species is one that alters community composition and whose presence is integral to the community structure (Paine, 1969). Migrating bison, through intense grazing, can influence the speed and duration of grassland green up (i.e. the green wave) across the landscape (Geremia et al., 2019). Mammoths altered the landscape by clearing trees, stripping bark, and digging thus increasing landscape heterogeneity, and possibly transforming environments from woodlands to grasslands (Haynes,

2012). Bison and mammoths are not only ecosystem engineers, but also keystone species. Both taxa could significantly modify the landscape and affect seasonal trends in vegetation growth and subsistence. Additionally, their behavior and associated landscape modification could have been vital to the continued presence of sympatric grassland species.

1.2. Ecological drivers of migration

There are few living analogues for fossil mammal movement patterns. Since there are no modern proboscideans in North America, I use savannah elephants as an analog for mammoth behavior. Alternatively, while many bison species went extinct during the Late Pleistocene, one species – *Bison bison* – survived and thus, is a suitable analog for the behavior of extinct bison.

Water availability is the most important driver of migration in African elephants (Chamaillé-Jammes et al., 2007; Harris et al., 2008; Loarie et al., 2009; Western, 1975; Western and Lindsay, 1984). At Amboseli National Park in Kenya, migration increased significantly during the wet season with over 40% of the population further than 10 kilometers (km) from the basin with some as far as 40km, while only 17% during the dry season (Western and Lindsay, 1984). In scenarios with abundant water sources, elephants tend to seek “areas with high vegetation cover” especially those with vast amounts of vegetation and adjacent areas with low vegetation cover (Harris et al., 2008). Migratory distances hypothesized for mammoths are highly variable with some studies suggesting distances between 200 and 500 km (Hoppe, 2004) and others claiming 500–1000 km (Churcher, 1980; Wooller et al., 2021). Comparatively, previous work has shown that elephants from Mali sometimes migrate over 3500 km in a single year (Wall et al., 2013). Since precipitation seasonality and vegetation cover are major factors affecting migration, it is probable that spatial, latitudinal, and temporal gradients in seasonality and vegetation richness affect the migration distance of both modern and fossil proboscideans.

The green wave hypothesis or the forage maturation hypothesis argues that herbivore migration is driven by waves of resource abundance and quality in the form of spring green-up (Fryxell et al., 1988; Van Der Graaf et al., 2006). Bison at Yellowstone follow the green wave during early spring, before slowing down and allowing the wave to pass them (Geremia et al., 2019). Furthermore, it has been shown that the intense grazing associated with increased densities “caused grasslands to green up faster, more intensely, and for a longer duration” (Geremia et al., 2019). These findings have led Geremia and colleagues (2019) to argue that while bison do migrate in response of forage quality, their own behavior engineers a portion of the green wave. Their claims have not been accepted without criticism, however, with some claiming that the Yellowstone bison migrate before the wave, allow it to pass them, and then follow it (Craine, 2020). Additional analyses suggest that bison migration tracks with the crest of the green wave for about half of spring, before “[regrazing] areas, which prolongs the period of maximized food quality and quantity” (Geremia et al., 2020).

Green wave surfing is seen in many herbivore taxa (e.g. elk, mule deer, and wildebeest) from North America, Europe, and Africa (Kauffman et al., 2021; Wilmshurst et al., 1999). This work suggests that the driving factors behind herbivore migration is consistent across the globe. However, the relationship between these driving factors and the migratory behaviors of Late Pleistocene bison and mammoths has yet to be confirmed. Migratory distance can be variable and could be associated with migration timing, anthropogenic risks, and winter residency as it is in mule deer (Sawyer et al., 2016). Sawyer and colleagues (2016) hypothesize that by reducing winter residency, long-distance migration mitigates the effects of competition for limited resources. While modern bison migration corridors at Yellowstone National Park tend to be under 100 kilometers (Geremia et al., 2020), this distance may be smaller than it was historically

due to anthropogenic constraints within the park and outside its boundaries. Additionally, the effect of water availability on bison migration remains contested due to conflicting evidence from GPS data (Allred et al., 2011) and stable isotope data (Hoppe, 2006).

1.3. Strontium isotopes

Strontium is a common element found throughout bedrock. Since ^{87}Sr is radioactive and is produced by the decay of ^{87}Rb (Faure, 1998, 1977), its concentration and its ratio relative to ^{86}Sr increases through time (Graustein, 1989). For example, pre-Cambrian bedrock tends have higher $^{87/86}\text{Sr}$ ratios than younger, Quaternary bedrock. Vegetation and groundwater incorporate strontium from their underlying weathering bedrock. Organisms incorporate strontium into their tissue from weathered bedrock in soil and water. However, most strontium in herbivores and omnivores comes from plant consumption (Price et al., 1985). Unlike other stable isotopes, strontium does not fractionate as it is incorporated into the biosphere and across food chains (Bataille et al., 2012). However, the $^{87/86}\text{Sr}$ ratios are affected by processes such as soil weathering and soil mixing (Bataille et al., 2012). Since strontium ratios reflect spatial variation in bedrock across a landscape, they can be used as a proxy of mobility in modern (Cerling et al., 2018; Singh et al., 2006; Van Der Merwe et al., 1990) and fossil fauna (Britton et al., 2009; Copeland et al., 2016; Esker et al., 2019; Hoppe, 2004; Hoppe and Koch, 2007).

1.4. Research questions and hypotheses

What were the driving factors behind mammoth and bison migration during the Late Pleistocene and early Holocene? If the bison in Pleistocene to Holocene central Texas behaved similarly to those from Yellowstone, we could expect their $^{87/86}\text{Sr}$ ratios to vary as they follow green waves towards the coast and display less variation when selecting areas to regaze. This

would likely result in bison $^{87/86}\text{Sr}$ ratios with limited (e.g. one or none) shifts in ratios, which we may also see during dry seasons as well (Allred et al., 2011; Hoppe, 2006). Mammoths may show a different pattern since their movement may be more strongly dependent on water availability than bison (Allred et al., 2011; Hoppe, 2006). Texas river basins have historically had two wet and dry seasons; however, this has shifted to one wet and dry season in modern time (Lee et al., 2017). Mammoths could travel further for improved forage quality when groundwater is abundant (i.e. during the wet season), while having a more restricted home range size and reduced forage quality when groundwater is less abundant (i.e. during the dry season). Isotopically, this could look like *Mammuthus* having multiple shifts in $^{87/86}\text{Sr}$ ratios associated with the cyclic wet and dry seasons. However, mammoths could have migrated considerable distances during the dry season if movement was associated with persistent rivers (Hoppe et al., 1999; Vereshchagin and Baryshnikov, 1991). Generally, mammoth $^{87/86}\text{Sr}$ ratios should display greater intratooth variation as compared to the bison species, resulting from variable home range sizes and a higher frequency of migration.

Did bison change their migratory patterns after the megafaunal extinctions? I hypothesize that as the mammoths migrated across Texas, they cleared trees, which would allow for the growth of new grasses, thus creating additional landscape heterogeneity. These would have included new areas for grasses, which would have been highly desirable for bison populations and as bison density increased in these areas, the timing and duration of spring green up would likely have increased as well. The mammoth populations would also benefit from this additional vegetation and would likely occupy an area on the ecotones of woodlands and grasslands. I predict that mammoths and bison had a semi-mutualistic and semi-competitive relationship in response to insufficient niche separation and that the mammoth extinction and bison diversity

collapse redefined the role of bison as ecosystem engineers in the Texas ecosystem. The effects of this change would likely be evident in the timing and duration of bison migration during the Holocene.

2. Materials and Methods

2.1. Materials

We serially sampled five mammoths and seven bison from before the majority of megafaunal extinctions (11,700 ka) and six bison from one site after the extinction event. All sampled teeth were excavated or collected from central Texas and stored at the Texas Memorial Museum in Vertebrate Paleontology. When possible, we selected teeth that had previously been bulk sampled for carbon and oxygen isotopes. We also included published, serially sampled strontium data for three mammoths and one bison from the Waco Mammoth National Monument in this study (Esker et al., 2019). However, this study followed a different higher-resolution enamel sampling protocol and thus, the time represented by each sample is slightly different. Since we assume that modern strontium variation in central Texas is not significantly different than prehistoric, we compiled modern strontium data from the geochemical literature to expand the existing Esker and colleagues (2019) isoscape of central Texas. This newly compiled data includes strontium values from multiple different substrates including vegetation, enamel, shells, and groundwater (Awwiller, 1994; Burke et al., 1982; Chesson et al., 2012; Christian et al., 2011; Cooke, 2005; Denison et al., 2003, 1998; Dennie, 2010; Dutton and Land, 1988; Dworkin and Land, 1994; Esker et al., 2019; Garcia-Fresca, 2004; Garrison et al., 1979; Goldberg, 2016; Goldberg and Griffith, 2017; Koepnick et al., 1985; Land et al., 1988; Moldovanyi et al., 1990; Musgrove et al., 2010; Musgrove and Banner, 2004; Oetting et al., 1996; Ohr et al., 1991; Otero

and Petri, 2010; Posey et al., 1987; Smith Enos and Kyle, 2002; Solis, 2020; Wiggins, 1986; Wong, 2013).

2.2. Methods

2.2.1. Predicting bison and mammoth migration corridors

Normalized Difference Vegetation Index (NDVI) is a measure of vegetation growth based on greenness from satellite imagery. The relationship between NDVI and vegetation productivity has been well documented in the literature (Asrar et al., 1984; Pettorelli et al., 2005; Sellers et al., 1992). NDVI is commonly used as a proxy for vegetation productivity to predict or quantify migration corridors (Bartlam-Brooks et al., 2013; Lendrum et al., 2014; Szép et al., 2006). In this study, I illustrate NDVI for the state of Texas between 1 Jan 2013 and 1 Jan 2014 (Figure 1). I used this animation to estimate the migration corridors associated with vegetation productivity in Central Texas based on the seasonal greenness of a particular region.

2.2.2. Enamel sampling

We followed a serial sampling protocol adapted from Hodgkins and colleagues (2020). Prior to sampling, all teeth were photographed to demonstrate extent of enamel removal. We applied isopropyl alcohol (70% alcohol by volume) to the surface of the tooth with a cotton swab. After waiting for it to dry, we removed dirt from an expanded area around the 2–4-millimeter horizontal bands from the cervix to the apex of the tooth. We then removed approximately 4-6 mg of enamel from a horizontal band along the tooth. In the case of the bison specimens, we assume an enamel growth rate for all teeth of about 55.4mm per year (Esker et al., 2019; Gadbury et al., 2000; Glassburn et al., 2018). When possible, we prioritized M2/M3 teeth (i.e. six months of enamel growth), however, in three cases, we did sample M1/M2s (i.e.

three months of enamel growth (Esker et al., 2019; Gadbury et al., 2000). We sampled the lobe of each molar five times from the cervix to the apex of the tooth, which represents approximately three to six months of enamel growth. For the mammoth specimens, we sampled the layer of aprismatic enamel along the enamel-dentine junction (Esker et al., 2019; Metcalfe and Longstaffe, 2012). Assuming an enamel growth rate of about 13 mm per year for mammoths (Dirks et al., 2012), we sampled each tooth seven times from the cervix to the apex of the tooth, which represents approximately one year of enamel growth. One specimen was only sampled three times, spanning almost two years of enamel growth, because most of the enamel was visibly degraded and may have been diagenetically altered. However, we focused sampling on areas that were not visibly degraded to reduce this effect.

2.2.3. Sample preparation and trace element analysis

All materials used for sample preparation (e.g. pipet tips, microcentrifuge tubes, vials, etc.) were pre-cleaned in boiling 50% nitric acid (HNO_3) for approximately 20 minutes and rinsed thrice with filtered deionized water from a GenPure end-polisher and thrice more with ultrapure water from a Savillex distiller. All sample preparation was done in a class 100 clean room at the University of Arkansas Radiogenic Isotope Laboratory.

All enamel samples were weighed out on a microbalance before being transferred to pre-cleaned microcentrifuge tubes. When possible, we utilized at least 2.5 mg of enamel, although this was not possible in some cases. Our enamel samples weighed between 0.96 and 5.912 mg. Due to the limited amount of enamel available, we did not pretreat our strontium powders (Funck et al., 2021; Widga et al., 2021). We then added 1 ml of 3.5N HNO_3 by weight (~1.092mg/mL). Samples were also prepared for trace element analysis if there were more than 2 mg of powder available, however, we did run one sample with a weight of 1.81 mg to ensure each tooth had a

trace element analysis in addition to strontium. A calculated portion of the digested enamel in the 3.5N HNO₃ solution was added to empty vials on a microbalance. The vials were then filled to 3 g with ultrapure water on the microbalance to make a 10,000 times diluted solution for trace element analysis. Trace element analyses followed Kamenov et al. (2018). Kamenov and colleagues concluded that V, Mn, Fe, La, Ce, Nd, Dy, Yb, Th, and U are useful elements for detecting diagenesis. All trace element samples were processed on an Thermo Scientific iCAP quadrupole inductively-coupled plasma mass spectrometer (iCAP Q ICP-MS). All trace element data was corrected to multiple concentrations of ICP-MS-68A, a commonly used standard that contained the desired trace elements. Following this, diluted strontium fractions were run to assess their concentrations before isotope analysis on the Nu Plasma HR multi-collector inductively-coupled plasma mass spectrometer (MC-ICP-MS). We also ran trace element blanks and an elemental standard (68A) at different concentrations throughout the run to monitor drift.

2.2.4. Column chemistry

Our column chemistry protocol followed Samuelsen (2020). Prior to running strontium columns, all columns were cleaned with 2 ml of triple-distilled water and then packed with about 100 microliters of Sr-spec resin. The columns were then conditioned with 1 ml of 3.5N HNO₃ before adding about 1000 microliters of our samples dissolved in HNO₃ into each column. After this, the sample was washed four times with 100 microliters of 3.5N HNO₃. The samples were washed one final time with 1 ml of 3.5N HNO₃. Finally, we added 1.98 ml of triple-distilled water to release the strontium from the resin into the vials along with an additional 0.03 ml of concentrated HNO₃. Blanks were prepared during this process to test for any contamination from our column chemistry protocol.

2.2.5. Strontium isotope ratio analysis

Following Samuelsen and Potra (2020) the strontium fractions were analyzed on a MC-ICP-MS with a desolvating system at the University of Arkansas' Trace Element and Radiogenic Isotope Laboratory (TRAIL). The MC-ICP-MS software documented any noticeable interference from Rb, Kr, and BaAr. After this, the strontium results were corrected to SRM 987 standard value ($^{87}\text{Sr}/^{86}\text{Sr} = 0.71025$). Blanks showed that our protocol generally did not introduce additional contamination and had no effect on the strontium results.

2.2.6. Geospatial modeling in ArcGIS Pro

Isoscapes are interpolated maps of strontium ratios across the landscape. They are used to estimate strontium variation in different areas to correlate to our enamel strontium ratios. We included strontium data from multiple different substrates (e.g. plants, animals with small ranges, water, and bedrock) to increase the resolution of the previous vegetation-based isoscape ($n = 36$) of central Texas. Before modeling, I reprojected our isoscape data points ($n = 594$) from WGS 1984 to a Texas State Plane system using a Lambert conformal conic projection. This was a necessary transformation to minimize scaling issues associated with the latitude and longitude coordinates in a global projection system. After reprojection, I interpolated strontium ratios for our study area using kriging in ArcGIS Pro with an output raster cell size of 500. Kriging was selected because it is a commonly used technique for producing isoscapes (Allen et al., 2018; Koehler et al., 2019; Lugli et al., 2022). Samples from across the geosphere (e.g. bedrock), hydrosphere (e.g. water) and biosphere (e.g. plants) are necessary to account for spatial variability. For example, water and vegetation samples from riparian regions serve as strontium baselines for highly mobile species associated with riparian resources (Bataille et al., 2020; Hamilton et al., 2019). Furthermore, there is negligible fractionation in strontium ratios across

the geosphere to biosphere suggesting that strontium ratios from large migratory mammals should directly reflect the strontium they consume from the biosphere and hydrosphere (Bataille et al., 2020). Ultimately, our isoscape correlates with the geologic map of Texas, thus reflecting the known relationship between strontium and age and lithology.

2.2.7. Two-member mixing models

Since each sample represents a relatively short period (e.g. days for bison and a week for mammoths), we use a two-member mixing model to estimate the amount of time spent in different areas for each sample. The two-member mixing model uses the following equation:

$$X_1 = \frac{R_{mix} - R_2}{R_1 - R_2} \times 100 \text{ (Faure, 1998, 1977).}$$

In this equation, X_1 is the percentage of time spent in strontium ratio associated with the fossil locality (where the fossil was recovered), R_{mix} is the observed strontium ratio in the enamel sample, R_1 is the strontium ratio for the fossil locality, and R_2 is the strontium ratio for a second locality. The two-localities selected for the model were the fossil locality (where the fossil was recovered) and a geologic region with a strontium ratio greater than the enamel sample (Esker et al., 2019). This mixing model represents the minimum distance travelled to develop the isotopic signatures associated with an individual enamel sample. An alternative, but similar mixing model was also used, which utilized strontium ratios associated with the fossil locality and the minimum or maximum strontium ratios on our isoscape. Minimum or maximum was selected based on whether the observed ratios from the dental sample were greater or less than the fossil locality ratios. I used these mixing models because even at the scale of days or a week, bison and mammoths were moving between multiple distinct strontium areas. These models were used to estimate the amount of time spent in each area. The Esker mixing model was reported in the results section with the alternative model in the appendix (Tables 2, 3, 4).

3. Results

3.1. Strontium Isoscape

The updated strontium isoscape (Figure 2) shows greater variation in the strontium ratios of central Texas geologic formations than previously estimated (Esker et al., 2019). This may be the result of greater resolution ($n = 594$) compared to the original isoscape ($n = 36$). It could also result from the inclusion of multiple strontium substrates including enamel, water, and bedrock. The fossil localities utilized in this study are located across multiple ecoregions: the Blackland Prairie ($n = 5$), eastern Cross Timbers ($n = 1$), or eastern Edwards Plateau ($n = 1$; Figure 3). The Blackland Prairie ecoregion at the northern part of Texas and the plains in southern Oklahoma are represented by a band of low strontium ratios between 0.70665 and 0.70891 (Figure 4). The coastal regions, associated with the Post Oak Savannah, Piney Woods, and Gulf Prairie ecoregions, are typically higher in strontium ratios between 0.70891 and 0.71100. There is a small Pre-Cambrian area with the Edwards Plateau into the Cross Timbers ecoregion with ratios closer to 0.71101 to 0.71690.

3.2. Pleistocene mammoth migration

The oldest mammoths included in this study are the Waco mammoths ($n = 3$) from Esker et al. (2019). These mammoths are dated to approximately 28 Ka and have been proposed to be a part of a single herd affected by a catastrophic event (Esker et al., 2019; Hoppe, 2004). Unlike the Pleistocene bison, mammoths demonstrate a substantial degree of intratooth variation. Mixing models suggest that all mammoths were associated with the Mesozoic deposits between 26-95% of the time: Mammoth 72's ratios suggest between 39 and 89%, Mammoth 318's ratios suggest 42 and 95%, and Mammoth 366's ratios suggest 26 and 94%. Mammoth 72 had a log-transformed standard deviation of $6.33e-4$ with Mammoth 318 at $6.32e-4$ and Mammoth 366 at

7.25e-4. These standard deviations are greater than the other Pleistocene mammoths sampled in this study.

Of the three mammoths sampled from Friesenhahn Cave, two (933-1505 and 933-2014) cluster together, while 933-2015 has a consistently higher strontium ratio. Mammoth 933-1505 has the highest log-transformed standard deviations ($\sim 3.83e-04$) and is the most variable of the Friesenhahn Cave mammoths. Mammoth 933-2014 has a log-transformed standard deviation of $2.28e-04$, while Mammoth 933-2015 has a log-transformed standard deviation of $2.20e-04$. A mixing model that at maximum, 933-1505's and 933-2014's, were associated with Mesozoic regions, surrounding Friesenhahn Cave, 62-68% of the time. The remainder of the strontium ratio (32-38%) was likely derived from the Cenozoic areas that have strontium ratios of ~ 0.711 . Comparatively, Mammoth 933-2015's ratios were associated less with the blue regions (42%) and more with the Cenozoic deposits (58%) with strontium ratios around 0.711. While the Esker model provides the most parsimonious explanation for how much time spent in different regions, in some cases, it could be possible for similar isotopic ratios to be produced ingesting resources from a region with an even higher isotopic signature, such as the Pre-Cambrian area around 75-100 kilometers from Austin, TX. This region's strontium ratio trends between 0.71309 and 0.71690. An alternative mixing model uses an average value for this region of 0.714995. In this mixing model, 83 to 90% of Mammoth 933-1505's strontium ratio was derived from the Mesozoic deposits similar to Mammoth 933-2015 (81%).

Unlike the Friesenhahn Cave mammoths, which likely incorporate strontium from different regions, the Congress Ave mammoths demonstrate relatively constrained strontium ratios. Their strontium ratios are most likely derived primarily from the Mesozoic deposits. The only shift from this pattern is in one of the five serial samples of Mammoth 43067-106; which

may be derived from Mesozoic deposits. The mixing models suggest that Mammoth 43067-37 derived 83 to 100% of its signal from the area around Congress Ave, while Mammoth 43067-106 likely derived between 71 to 100% of its signal from this area. The log-transformed standard deviations for both Mammoth 43067-37 ($\sim 8.46e-05$) and Mammoth 43067-106 ($\sim 1.19e-04$) are lower than the Friesenhahn Cave and Waco mammoths. Unlike the Friesenhahn Cave and Waco mammoths, the Congress Ave mammoths have little intratooth variation, which is a similar pattern to the Friesenhahn Cave bison. None of our individuals show ratios as high as the Pre-Cambrian area, suggesting a lack of movement from central Texas to western Texas during our study period.

3.3. Pleistocene bison migration

The oldest bison samples derive from Leo Boatright Pit ($n = 1$) and Valley Farms ($n = 1$), which are dated to between 70 to 30 Ka and are located less than 50 km from each other. The bison from Leo Boatright Pit has strontium ratios inconsistent with the ratios of the fossil site (Figure 4). The two-member mixing models show that this individual derived 90 to 100% of its strontium ratio from the Mesozoic deposits, which may also range into Oklahoma. This bison features the smallest standard deviation of any samples in this study ($\sim 3.25e-05$), suggesting a relatively limited seasonal variation. The bison from Valley Farms also has limited log-transformed standard deviations suggesting low seasonal variation ($\sim 5.13e-05$). The Valley Farms bison also appears to have derived most of its strontium signal from the Mesozoic deposits with slightly higher strontium ratios than the Leo Boatright Pit bison. The two-member mixing models confirms that this individual derived 88 and 100% of its signal from the Mesozoic deposits.

Unlike Leo Boatright Pit and Valley Farms, which are both in the Blackland Prairie ecoregion, Waco Mammoth National Monument is the only fossil locality sampled from the Cross Timbers ecoregion. The Waco bison dates to approximately 28 Ka and derived its strontium ratio from Cenozoic deposits of the isoscape (between 61 to 100%). Unlike the Leo Boatright Pit and Valley Farms bison, the Waco bison's strontium ratios vary substantially between samples with a significant dip in the middle of the tooth (Figure 9). Its log-transformed standard deviation is approximately $4.69e-4$, which is larger than Leo Boatright Pit and Valley Farms. However, these samples come from a published study, which followed a different sampling strategy (Esker et al., 2019).

Friesenhahn Cave is the only locality where both bison ($n = 4$) and mammoths ($n = 3$) are represented, and it is dated to between 20 and 17.8 Ka. Three of the four bison at Friesenhahn Cave cluster together within the local range (~50 km) around the cave with one bison having a distinct strontium ratio (Figure 8). The mixing models suggest that the majority of the Friesenhahn Cave bison (933-2198, 933-3390, 933-3403) were associated with the Mesozoic deposits 74 to 96% of their time. The other Friesenhahn Cave bison sampled (933-3285) likely derived 31 to 85% of its strontium ratio from the Mesozoic deposits. Friesenhahn Cave bison 933-2198 ($\sim 1.64e-04$) and 933-3285 ($\sim 6.36e-04$) display greater occurrences of log-transformed standard deviation than Friesenhahn Cave bison 933-3390 ($\sim 6.02e-05$) and 933-3403 ($9.45e-05$). Friesenhahn Cave bison 933-3285 has the highest levels of log-transformed standard deviation of all Pleistocene samples, including mammoths and bison.

Cave Without A Name is a Terminal Pleistocene site and is dated to 11 Ka (Table 1). We sampled one bison from the cave. Its strontium ratios are largely comparable to specimens from Leo Boatright Pit, Valley Farms, and three of the four Friesenhahn Cave bison. The mixing

models suggest that the bison spent between 91 and 100% of its time in the Mesozoic deposits. As compared with the Valley Farms and Leo Boatright Pit bison, it displays a gradual trend, from older to younger, towards the Mesozoic area. The standard deviation for this bison ($\sim 1.69e-04$) is the third highest of the Pleistocene bison sampled, only lower than the Friesenhahn Cave 3285 bison and Waco 1190 bison. As time progresses towards the Terminal Pleistocene, there appears to be a gradual increase in bison strontium ratio standard deviations with the Waco bison as an extremely variable outlier, likely reflecting differences in sampling protocols.

3.4. Holocene bison migration

The Holocene bison samples ($n = 6$) come from 77 Ranch; a site estimated to be early Holocene (Figure 7). These samples show a considerably greater range in their strontium ratios compared to any of the Pleistocene bison sites. The largest cluster ($n = 3$) derived most of their strontium signal from the Cenozoic coastal deposits. The mixing models suggest that most of the Holocene bison derived less of their signals from the Mesozoic bands compared to the Pleistocene bison. Instead, they may have derived a significant amount of their signal from the Cenozoic area east of the site. One bison (45817-158) appears to have derived the majority of its three-six month signal from Cenozoic deposits before moving to the Mesozoic deposits and then returning to the Cenozoic deposits no more than a month later. This bison has the highest standard deviation ($\sim 4.653708e-04$) observed for any sampled bison in both the Pleistocene and Holocene. Most of the 77 Ranch bison have higher standard deviations than the Pleistocene bison, suggesting a greater seasonal movement or greater variability not captured in the isoscape.

4. Discussion

4.1. Paleoclimate of central Texas during the Late Pleistocene and early Holocene

Limited research has been done on regional-scale paleoclimate of central Texas during the Late Pleistocene and early Holocene. However, previous work has demonstrated that eastern Texas was dominated by “Poaceae, Cyperaceae, and Asteraceae pollen together with significant representation of Pinus, Alnus, and Picea at Patschke Bog” during the Last Glacial Maximum (Jackson et al., 2000). Those pollen taxa are commonly associated with open environments. Additional paleoethnobotanical work has also suggested that at least part of the Edwards Plateau surrounding Halls Cave was associated with open environments after the LGM (18-16 Ka; Cordova and Johnson, 2019). Multiple palynological studies have argued that modern analog environments do not exist for Pleistocene Texas (Bousman, 1998; Jackson et al., 2000). However, despite the lack of modern analogs, this open environment paleoclimatic reconstruction of eastern Texas favors a west to east migration corridors for the bison and mammoths during the Pleistocene. The west to east corridor is also supported by modern seasonal vegetation productivity changes indicated by NDVI (Fig.1), although this could have varied historically. The palynological evidence from central Texas suggests that the composition of woodland communities, once dominating the landscape during the Late Pleistocene, changed dramatically during the early Holocene with a significant reduction in canopy cover by 7000 BP (Bousman, 1998). Palynological work at Halls Cave suggests that arboreal vegetation increases during the early Holocene, but it is accompanied by dry grasses, which could suggest aridification in the early Holocene that might affect bison behavior (Cordova and Johnson, 2019). This expansion of open and wooded grasslands is consistent with the expansion of bison

migration corridors during the early Holocene, which could suggest that climate was a driving factor behind the observed shift in migratory patterns.

4.2. Pleistocene migration corridors

During the Pleistocene, our models show that bison were generally only migrating within the Mesozoic area, which corresponds primarily with the Blackland Prairie regions of Texas, with little to no time incorporating resources from Cenozoic deposits associated with the Gulf Prairies and Piney Woods ecoregions. Even within the prairie ecoregions, numerous specimens appear to be constrained within particular regions of the Blackland Prairie ecoregion that is primarily north-south in extent. These results suggest that that bison migration corridors were relatively constrained during the Pleistocene in central Texas. Additional data is necessary to identify the specific causal agents responsible for the constrained nature of Pleistocene bison ranges. A single individual (Specimen 933-3285) from Friesenhahn cave incorporated strontium from a region that was beyond the Blackland Prairie region before ultimately returning to the area before death, reminding us that individual patterns could differ from community-scale trends in some cases. Additionally, this individual could also suggest that lifetime patterns of movement may differ from those recorded in early life in an animal's teeth. This individual differs from other Pleistocene bison and mammoth by traveling at least 50 kilometers from Friesenhahn Cave into some Cenozoic deposits.

Mammoth strontium ratios vary more during the Pleistocene, which could be driven by spatially and/or temporal differences in environment. The strontium patterns of individuals at Congress Ave and Friesenhahn Cave are internally consistent and vary strongly between sites. The sites are separated by 100 km and estimated to be separated by ~5,000 years in age. While Mammoth 933-2014's strontium ratios are similar to Mammoth 933-1505, it displays less

intratooth variation, suggesting lower seasonal variation in movement. Mixing models suggest that the Congress Ave individuals incorporated most of their signal from the Mesozoic, prairie areas and had likely incorporated minimal resources from the Cenozoic regions, the majority of which are associated with coastal riparian habitats. Alternatively, the Friesenhahn Cave mammoths incorporate significant amounts of their signal from several different areas and display more seasonal variation than is observed in the Congress Ave mammoths and nearly all of the Pleistocene bison. This seasonal variation resembles what we observed for the Holocene bison from 77 Ranch. The mammoths from Friesenhahn Cave travelled at least 50km from the where they died to acquire their isotopic signatures. Additionally, these corridors could be consistent with traveling along the San Antonio or Guadalupe Rivers that are spatially associated with Friesenhahn Cave.

Mixing models suggest that the Congress Ave mammoths are constrained within the Mesozoic, prairie areas; this is consistent with minimal seasonal movement or movement from north to south within the prairie ecoregion. While a primarily Blackland Prairie migratory corridor is a consistent interpretation for Pleistocene bison, this is not the case for Friesenhahn Cave mammoths. While Congress Ave is less than 100 km from Friesenhahn Cave, the estimated ages of the sites overlap, where Congress Ave is dated to 19-15 and Friesenhahn Cave dated to 20-17.8 Ka (Table 1). The younger age estimates for the Congress Ave site could associate these individuals with the increasing temperatures before the Bølling-Allerød decreased water availability, resulting in a reduction in mammoth home range sizes at Congress Ave. Furthermore, the colder temperatures associated with the Last Glacial Maximum (25-19 ka) likely increased water availability (Marshall and Clarke, 1999) and consequently, mammoth home range sizes. The constrained inter-tooth ratios from Congress Ave challenges the interpretation that

mammoths are may be tied to riparian corridors, which follow an east-west trajectory and instead suggests that mammoth migration may have been either spatially or temporally variable.

4.3. Holocene migration corridors

During the Holocene, the bison appear to incorporate strontium from regions beyond the Mesozoic areas favored by Pleistocene bison, incorporating strontium from the Cenozoic areas. This could suggest that following the mammoth extinctions, bison began exploiting the rich, riparian areas towards coastal Texas Rather than having constrained movement or primarily north-south movement. However, these results could also be consistent with increased aridity during the Holocene, possibly driving additional bison migration. This change in behavior is consistent with the variable strontium ratios found in mammoth samples, and inconsistent with most of the Pleistocene bison strontium results. However, 77 Ranch is thought to be an alluvial site and thus, could be composed of individuals from a broader range of localities than the cave and pit assemblages that comprise Pleistocene samples (77 Ranch Field Notes). Despite this, two of the six bison sampled resemble those from the nearby Pleistocene sites (Leo Boatright Pit and Valley Farms), while the other individuals show considerably more variation within each of their dentition. Mixing models suggest that it would be necessary to incorporate strontium from regions as far as 75 kilometers from where they died to develop their isotopic signatures. However, one of bison individual may have returned to the area around 77 Ranch from Cenozoic deposits during the period recorded in this study. Further, despite the site's proximity to Leo Boatright Pit and Valley Farms (< 50 km), 77 Ranch individuals show substantially more intratooth variation compared to the Pleistocene bison individuals. On average, Holocene bison strontium ratios suggest that their ranges may have expanded during the early Holocene, which could be a direct response to the megafaunal extinctions or to the climatic shifts and expanding

human populations during this time. An alternative interpretation is that the variation seen at 77 Ranch results from it being alluvially accumulated site and thus, could represent spatial variation, rather than temporal. However, this interpretation fails to address the greater tooth variation within individuals and rather, supports the idea that this possibly is a widespread signal across multiple populations in the Holocene.

4.4. Landscape of fear: human impacts on post-extinction communities

Humans appear to have quickly become a keystone species, ecosystem engineer, and, similarly to African hunter-gatherers, niche constructors in North America (Pinter et al., 2011; Thompson et al., 2021). While the causes of megafaunal extinction in North America remains highly contested, it is abundantly clear that human behavior could have had cascading effects on faunal behavior (Becerra-Valdivia and Higham, 2020; Broughton and Weitzel, 2018; Bustos et al., 2018). Furthermore, modern work has demonstrated that the increasing human footprint is a major variable in African elephant home range size and distribution (Wall et al., 2021).

5. Conclusion

Using modern bison behavior as an analog for Pleistocene bison, we predicted that the Pleistocene bison would generally orient themselves along a west-east gradient to follow the phenological gradients across eastern Texas, but instead they have either highly constrained movement patterns, or they oriented themselves north-south following an alternative gradient of vegetation along the plains in Texas and/or Oklahoma that does not appear to be highly seasonally variable today (NDVI fig.). This pattern appears to change in the Holocene with an increase in bison intratooth variation and the presence of additional migration corridors. These corridors led to both the Mesozoic and Cenozoic areas, unlike the previously dominant migration

corridors only within the Mesozoic areas during the Pleistocene. Future work will focus on paleoclimatic reconstructions of central Texas to attempt to identify the causal agent(s) driving these changes in bison migration corridors. We hypothesized a similar west-east pattern for the mammoths and while this hypothesis is consistent with the inter-tooth strontium ratios of individuals from Friesenhahn Cave and Waco, we saw a different pattern at Congress Ave. There mammoths are either spatially constrained or follow a spatially restricted north-south movement pattern, suggesting heterogeneity in mammoth migratory behavior at a spatial or temporal scale. Thus, the Congress Ave mammoths may contradict the hypothesis derived from modern African elephants, that all mammoths should show large amounts of variation in strontium incorporation. However, additional climatic reconstructions at Congress Ave and Friesenhahn Cave are needed to address whether the observed relationship is a product of spatial or temporal variation. Clarifying the chronology of 77 Ranch and sampling additional Pleistocene and Holocene bison and mammoths from coastal Texas would test the broader implications of our findings.

References

- Allen, S.T., Kirchner, J.W., Goldsmith, G.R., 2018. Predicting Spatial Patterns in Precipitation Isotope ($\delta^2\text{H}$ and $\delta^{18}\text{O}$) Seasonality Using Sinusoidal Isoscapes. *Geophys. Res. Lett.* 45, 4859–4868. <https://doi.org/10.1029/2018GL077458>
- Allred, B.W., Fuhlendorf, S.D., Hamilton, R.G., 2011. The role of herbivores in Great Plains conservation: Comparative ecology of bison and cattle. *Ecosphere* 2, 1–17. <https://doi.org/10.1890/ES10-00152.1>
- Asrar, G., Fuchs, M., Kanemasu, E.T., Hatfield, J.L., 1984. Estimating Absorbed Photosynthetic Radiation and Leaf Area Index from Spectral Reflectance in Wheat. *Agron. J.* 76, 300–306. <https://doi.org/10.2134/agronj1984.00021962007600020029x>
- Awwiller, D.N., 1994. Geochronology and mass transfer in Gulf Coast mudrocks (south–central Texas, USA): Rb–Sr, Sm–Nd and REE systematics. *Chem. Geol.* 116, 61–84.
- Bartlam-Brooks, H.L.A., Beck, P.S.A., Bohrer, G., Harris, S., 2013. In search of greener pastures: Using satellite images to predict the effects of environmental change on zebra migration. *J. Geophys. Res. Biogeosciences* 118, 1427–1437. <https://doi.org/10.1002/jgrg.20096>
- Bataille, C.P., Crowley, B.E., Wooller, M.J., Bowen, G.J., 2020. Advances in global bioavailable strontium isoscapes. *Palaeogeogr. Palaeoclimatol. Palaeoecol.* 555, 109849. <https://doi.org/10.1016/j.palaeo.2020.109849>
- Bataille, C.P., Laffoon, J., Bowen, G.J., 2012. Mapping multiple source effects on the strontium isotopic signatures of ecosystems from the circum-Caribbean region. *Ecosphere* 3, art118. <https://doi.org/10.1890/es12-00155.1>
- Becerra-Valdivia, L., Higham, T., 2020. The timing and effect of the earliest human arrivals in North America. *Nature* 584, 93–97. <https://doi.org/10.1038/s41586-020-2491-6>
- Bousman, C.B., 1998. Paleoenvironmental change in Central Texas: The palynological evidence. *Plains Anthropol.* 43, 201–219. <https://doi.org/10.1080/2052546.1998.11931900>
- Britton, K., Grimes, V., Dau, J., Richards, M.P., 2009. Reconstructing faunal migrations using intra-tooth sampling and strontium and oxygen isotope analyses: a case study of modern caribou (*Rangifer tarandus granti*). *J. Archaeol. Sci.* 36, 1163–1172. <https://doi.org/10.1016/j.jas.2009.01.003>
- Broughton, J.M., Weitzel, E.M., 2018. Population reconstructions for humans and megafauna suggest mixed causes for North American Pleistocene extinctions. *Nat. Commun.* 9, 1–12. <https://doi.org/10.1038/s41467-018-07897-1>
- Burke, W.H., Denison, R.E., Hetherington, E.A., Koepnick, R.B., Nelson, H.F., Otto, J.B., 1982.

- Variation of seawater $^{87}\text{Sr}/^{86}\text{Sr}$ throughout Phanerozoic time. *Geology* 10, 516–519. [https://doi.org/10.1130/0091-7613\(1982\)10<516:VOSSTP>2.0.CO;2](https://doi.org/10.1130/0091-7613(1982)10<516:VOSSTP>2.0.CO;2)
- Bustos, D., Jakeway, J., Urban, T.M., Holliday, V.T., Fenerty, B., Raichlen, D.A., Budka, M., Reynolds, S.C., Allen, B.D., Love, D.W., Santucci, V.L., Odess, D., Willey, P., McDonald, H.G., Bennett, M.R., 2018. Footprints preserve terminal Pleistocene hunt? Human-sloth interactions in North America. *Sci. Adv.* 4, 1–7. <https://doi.org/10.1126/sciadv.aar7621>
- Cerling, T.E., Andanje, S.A., Gakuya, F., Kariuki, J.M., Kariuki, L., Kingoo, J.W., Khayale, C., Lekolool, I., Macharia, A.N., Anderson, C.R., Fernandez, D.P., Hu, L., Thomas, S.J., 2018. Stable isotope ecology of black rhinos (*Diceros bicornis*) in Kenya. *Oecologia* 187, 1095–1105. <https://doi.org/10.1007/s00442-018-4185-4>
- Chamailé-Jammes, S., Valeix, M., Fritz, H., 2007. Managing heterogeneity in elephant distribution: Interactions between elephant population density and surface-water availability. *J. Appl. Ecol.* 44, 625–633. <https://doi.org/10.1111/j.1365-2664.2007.01300.x>
- Chesson, L.A., Tipple, B.J., Mackey, G.N., Hynek, S.A., Fernandez, D.P., Ehleringer, J.R., 2012. Strontium isotopes in tap water from the coterminous USA. *Ecosphere* 3, art67. <https://doi.org/10.1890/es12-00122.1>
- Christian, L.N., Banner, J.L., Mack, L.E., 2011. Sr isotopes as tracers of anthropogenic influences on stream water in the Austin, Texas, area. *Chem. Geol.* 282, 84–97. <https://doi.org/10.1016/j.chemgeo.2011.01.011>
- Churcher, C.S., 1980. Did the North American mammoth migrate? *Can. J. Anthropol.* 1, 103–105.
- Cooke, M.J., 2005. Soil formation and erosion in central Texas: Insights from relict soils and cave deposits.
- Copeland, S.R., Cawthra, H.C., Fisher, E.C., Lee-Thorp, J.A., Cowling, R.M., le Roux, P.J., Hodgkins, J., Marean, C.W., 2016. Strontium isotope investigation of ungulate movement patterns on the Pleistocene Paleo-Agulhas Plain of the Greater Cape Floristic Region, South Africa. *Quat. Sci. Rev.* <https://doi.org/10.1016/j.quascirev.2016.04.002>
- Cordova, C.E., Johnson, W.C., 2019. An 18 ka to present pollen-and phytolith-based vegetation reconstruction from Hall’s Cave, south-central Texas, USA. *Quat. Res. (United States)* 92, 497–518. <https://doi.org/10.1017/qua.2019.17>
- Craine, J.M., 2020. Mischaracterization of bison migratory patterns in Yellowstone National Park: Consequences for the green wave hypothesis. *Proc. Natl. Acad. Sci. U. S. A.* 117, 9169–9170. <https://doi.org/10.1073/pnas.1920842117>
- Denison, R.E., Kirkland, D.W., Evans, R., 1998. Using strontium isotopes to determine the age and origin of gypsum and anhydrite beds. *J. Geol.* 106, 1–17.

<https://doi.org/10.1086/515996>

- Denison, R.E., Miller, N.R., Scott, R.W., Reaser, D.F., 2003. Strontium isotope stratigraphy of the Comanchean Series in north Texas and southern Oklahoma. *Bull. Geol. Soc. Am.* 115, 669–682. [https://doi.org/10.1130/0016-7606\(2003\)115<0669:SISOTC>2.0.CO;2](https://doi.org/10.1130/0016-7606(2003)115<0669:SISOTC>2.0.CO;2)
- Dennie, D.P., 2010. An integrated paleomagnetic and diagenetic investigation of the Barnett shale and underlying Ellenburger Group carbonates, Fort Worth Basin, Texas.
- Dirks, W., Bromage, T.G., Agenbroad, L.D., 2012. The duration and rate of molar plate formation in *Palaeoloxodon cypriotes* and *Mammuthus columbi* from dental histology. *Quat. Int.* 255, 79–85. <https://doi.org/10.1016/j.quaint.2011.11.002>
- Dutton, S.P., Land, L.S., 1988. Cementation and Burial History of a Low-Permeability Quartzarenite, Lower Cretaceous Travis Peak Formation, East Texas. *Bull. Geol. Soc. Am.* 100, 1271–1282. [https://doi.org/10.1130/0016-7606\(1988\)100<1271:CABHOA>2.3.CO;2](https://doi.org/10.1130/0016-7606(1988)100<1271:CABHOA>2.3.CO;2)
- Dworkin, S.I., Land, L.S., 1994. Petrographic and geochemical constraints on the formation and diagenesis of anhydrite cements, Smackover sandstones, Gulf of Mexico. *J. Sediment. Res. A Sediment. Petrol. Process.* 64 A, 339–348. <https://doi.org/10.1306/d4267d98-2b26-11d7-8648000102c1865d>
- Esker, D., Forman, S.L., Widga, C., Walker, J.D., Andrew, J.E., 2019. Home range of the Columbian mammoths (*Mammuthus columbi*) and grazing herbivores from the Waco Mammoth National Monument, (Texas, USA) based on strontium isotope ratios from tooth enamel bioapatite. *Palaeogeogr. Palaeoclimatol. Palaeoecol.* 534, 109291. <https://doi.org/10.1016/j.palaeo.2019.109291>
- Faure, G., 1998. Mixing Models, in: *Principles and Applications of Geochemistry: A Comprehensive Textbook for Geology Students.* pp. 328–341.
- Faure, G., 1977. Strontium in two-component mixtures, in: *Principles of Isotope Geology.* John Wiley & Sons, pp. 97–105.
- Fryxell, J.M., Greever, J., Sinclair, A.R.E., 1988. Why are migratory ungulates so abundant? *Am. Nat.* 131, 781–798. <https://doi.org/10.1086/284822>
- Funck, J., Bataille, C., Rasic, J., Wooller, M., 2021. A bio-available strontium isoscape for eastern Beringia: a tool for tracking landscape use of Pleistocene megafauna. *J. Quat. Sci.* 36, 76–90. <https://doi.org/10.1002/jqs.3262>
- Gadbury, C., Todd, L., Jahren, A.H., Amundson, R., 2000. Spatial and temporal variations in the isotopic composition of bison tooth enamel from the Early Holocene Hudson-Meng Bone Bed, Nebraska. *Palaeogeogr. Palaeoclimatol. Palaeoecol.* 157, 79–93. [https://doi.org/10.1016/S0031-0182\(99\)00151-0](https://doi.org/10.1016/S0031-0182(99)00151-0)

- Garcia-Fresca, B., 2004. Urban effects on groundwater recharge in Austin, Texas.
- Garrison, J.R., Long, L.E., Richmann, D.L., 1979. Rb-Sr and K-Ar geochronologic and isotopic studies, Llano Uplift, central Texas. *Contrib. to Mineral. Petrol.* 69, 361–374. <https://doi.org/10.1007/BF00372262>
- Geremia, C., Merkle, J.A., Eacker, D.R., Wallen, R.L., White, P.J., Hebblewhite, M., Kauffman, M.J., 2019. Migrating bison engineer the green wave. *Proc. Natl. Acad. Sci. U. S. A.* 116, 25707–25713. <https://doi.org/10.1073/pnas.1913783116>
- Geremia, C., Merkle, J.A., White, P.J., Hebblewhite, M., Kauffman, M.J., 2020. Reply to craine: Bison redefine what it means to move to find food. *Proc. Natl. Acad. Sci. U. S. A.* 117, 9171–9172. <https://doi.org/10.1073/pnas.2000713117>
- Glassburn, C.L., Potter, B.A., Clark, J.L., Reuther, J.D., Bruning, D.L., Wooller, M.J., 2018. Strontium and oxygen isotope profiles of sequentially sampled modern bison (Bison bison) teeth from interior alaska as proxies of seasonal mobility. *Arctic* 71, 183–200. <https://doi.org/10.14430/arctic4718>
- Goldberg, R.B., 2016. $^{87}\text{Sr}/^{86}\text{Sr}$ as a Potential Fingerprint for Determining the Provenance Of Total Dissolved Solids Associated With Hydraulic Fracturing Activities in the Barnett Shale, Texas.
- Goldberg, R.B., Griffith, E.M., 2017. Strontium isotopes as a potential fingerprint of total dissolved solids associated with hydraulic-fracturing activities in the Barnett Shale, Texas. *Environ. Geosci.* 24, 151–165. <https://doi.org/10.1306/eg.06191716501>
- Graustein, W.C., 1989. $^{87}\text{Sr}/^{86}\text{Sr}$ Ratios Measure the Sources and Flow of Strontium in Terrestrial Ecosystems, in: *Stable Isotopes in Ecological Research*. pp. 491–512.
- Hamilton, M., Nelson, S. V., Fernandez, D.P., Hunt, K.D., 2019. Detecting riparian habitat preferences in “savanna” chimpanzees and associated Fauna with strontium isotope ratios: Implications for reconstructing habitat use by the chimpanzee-human last common ancestor. *Am. J. Phys. Anthropol.* 170, 551–564. <https://doi.org/10.1002/ajpa.23932>
- Harris, G.M., Russell, G.J., Van Aarde, R.I., Pimm, S.L., 2008. Rules of habitat use by elephants *Loxodonta africana* in southern Africa: Insights for regional management. *Oryx* 42, 66–75. <https://doi.org/10.1017/S0030605308000483>
- Haynes, G., 2012. Elephants (and extinct relatives) as earth-movers and ecosystem engineers. *Geomorphology* 157–158, 99–107. <https://doi.org/10.1016/j.geomorph.2011.04.045>
- Hoppe, K.A., 2006. Correlation between the oxygen isotope ratio of North American bison teeth and local waters: Implication for paleoclimatic reconstructions. *Earth Planet. Sci. Lett.* 244, 408–417. <https://doi.org/10.1016/j.epsl.2006.01.062>

- Hoppe, K.A., 2004. Late Pleistocene mammoth herd structure, migration patterns, and Clovis hunting strategies inferred from isotopic analyses of multiple death assemblages. *Paleobiology* 30, 129–145. [https://doi.org/10.1666/0094-8373\(2004\)030<0129:lpmhsm>2.0.co;2](https://doi.org/10.1666/0094-8373(2004)030<0129:lpmhsm>2.0.co;2)
- Hoppe, K.A., Koch, P.L., 2007. Reconstructing the migration patterns of late Pleistocene mammals from northern Florida, USA. *Quat. Res.* 68, 347–352. <https://doi.org/10.1016/j.yqres.2007.08.001>
- Hoppe, K.A., Koch, P.L., Carlson, R.W., Webb, S.D., 1999. Tracking mammoths and mastodons: Reconstruction of migratory behavior using strontium isotope ratios. *Geology* 27, 439–442. [https://doi.org/10.1130/0091-7613\(1999\)027<0439:TMAMRO>2.3.CO;2](https://doi.org/10.1130/0091-7613(1999)027<0439:TMAMRO>2.3.CO;2)
- Jackson, S.T., Webb, R.S., Anderson, K.H., Overpeck, J.T., Webb, T., Williams, J.W., Hansen, B.C.S., 2000. Vegetation and environment in eastern North America during the Last Glacial Maximum. *Quat. Sci. Rev.* 19, 489–508. [https://doi.org/10.1016/S0277-3791\(99\)00093-1](https://doi.org/10.1016/S0277-3791(99)00093-1)
- Jones, C.G., Lawton, J.H., Shackak, M., 1994. Organisms as Ecosystem Engineers. *Oikos* 69, 373–386.
- Kamenov, G.D., Lofaro, E.M., Goad, G., Krigbaum, J., 2018. Trace elements in modern and archaeological human teeth: Implications for human metal exposure and enamel diagenetic changes. *J. Archaeol. Sci.* 99, 27–34. <https://doi.org/10.1016/j.jas.2018.09.002>
- Kauffman, M.J., Cagnacci, F., Chamaillé-Jammes, S., Hebblewhite, M., Hopcraft, J.G.C., Merkle, J.A., Mueller, T., Mysterud, A., Peters, W., Roettger, C., Steingisser, A., Meacham, J.E., Abera, K., Adamczewski, J., Aikens, E.O., Bartlam-Brooks, H., Bennitt, E., Berger, J., Boyd, C., Côté, S.D., Debeffe, L., Dekrout, A.S., Dejid, N., Donadio, E., Dziba, L., Fagan, W.F., Fischer, C., Focardi, S., Fryxell, J.M., Fynn, R.W.S., Geremia, C., González, B.A., Gunn, A., Gurarie, E., Heurich, M., Hilty, J., Hurley, M., Johnson, A., Joly, K., Kaczensky, P., Kendall, C.J., Kochkarev, P., Kolpaschikov, L., Kowalczyk, R., Langevelde, F. Van, Li, B. V., Lobora, A.L., Loison, A., Madiri, T.H., Mallon, D., Marchand, P., Medellin, R.A., Meisingset, E., Merrill, E., Middleton, A.D., Monteith, K.L., Morjan, M., Morrison, T.A., Mumme, S., Naidoo, R., Novaro, A., Ogutu, J.O., Olson, K.A., Oteng-Yeboah, A., Ovejero, R.J.A., Owen-Smith, N., Paasivaara, A., Packer, C., Panchenko, D., Pedrotti, L., Plumptre, A.J., Rolandsen, C.M., Said, S., Salemgareyev, A., Savchenko, A., Savchenko, P., Sawyer, H., Selebatso, M., Skroch, M., Solberg, E., Stabach, J.A., Strand, O., Sutor, M.J., Tachiki, Y., Trainor, A., Tshipa, A., Virani, M.Z., Vynne, C., Ward, S., Wittemyer, G., Xu, W., Zuther, S., 2021. Mapping out a future for ungulate migrations. *Science* (80-.). 372, 566–569. <https://doi.org/10.1126/science.abf0998>
- Koch, P.L., Barnosky, A.D., 2006. Late quaternary extinctions: State of the debate. *Annu. Rev. Ecol. Evol. Syst.* 37, 215–250. <https://doi.org/10.1146/annurev.ecolsys.34.011802.132415>
- Koch, P.L., Diffenbaugh, N.S., Hoppe, K.A., 2004. The effects of late Quaternary climate and pCO₂ change on C 4 plant abundance in the south-central United States. *Palaeogeogr.*

- Palaeoclimatol. Palaeoecol. 207, 331–357. <https://doi.org/10.1016/j.palaeo.2003.09.034>
- Koehler, G., Kardynal, K.J., Hobson, K.A., 2019. Geographical assignment of polar bears using multi-element isoscapes. *Sci. Rep.* 9, 1–9. <https://doi.org/10.1038/s41598-019-45874-w>
- Koepnick, R.B., Burke, W.H., Denison, R.E., Hetherington, E.A., Nelson, H.F., Otto, J.B., Waite, L.E., 1985. Construction of the seawater $^{87}\text{Sr}/^{86}\text{Sr}$ curve for the cenozoic and cretaceous: Supporting data. *Chem. Geol. Isot. Geosci. Sect.* 58, 55–81.
- Land, L.S., Macpherson, G.L., Mack, L.E., 1988. The Geochemistry of Saline Formation Waters, Miocene, Offshore Louisiana. *Gulf Coast Assoc. Geol. Soc. Trans.* 38, 503–511.
- Lee, K., Gao, H., Huang, M., Sheffield, J., Shi, X., 2017. Development and Application of Improved Long-Term Datasets of Surface Hydrology for Texas. *Adv. Meteorol.* 2017. <https://doi.org/10.1155/2017/8485130>
- Lendrum, P.E., Anderson, C.R., Monteith, K.L., Jenks, J.A., Bowyer, R.T., 2014. Relating the movement of a rapidly migrating ungulate to spatiotemporal patterns of forage quality. *Mamm. Biol.* 79, 369–375. <https://doi.org/10.1016/j.mambio.2014.05.005>
- Loarie, S.R., Aarde, R.J.V., Pimm, S.L., 2009. Fences and artificial water affect African savannah elephant movement patterns. *Biol. Conserv.* 142, 3086–3098. <https://doi.org/10.1016/j.biocon.2009.08.008>
- Lugli, F., Cipriani, A., Bruno, L., Ronchetti, F., Cavazzuti, C., Benazzi, S., 2022. A strontium isotope of Italy for provenance studies. *Chem. Geol.* 587, 120624. <https://doi.org/10.1016/j.chemgeo.2021.120624>
- Marshall, S.J., Clarke, G.K.C., 1999. Modeling North American Freshwater Runoff through the Last Glacial Cycle. *Quat. Res.* 52, 300–315.
- Metcalf, J.Z., Longstaffe, F.J., 2012. Mammoth tooth enamel growth rates inferred from stable isotope analysis and histology. *Quat. Res.* 77, 424–432. <https://doi.org/10.1016/j.yqres.2012.02.002>
- Moldovanyi, E.P., Walter, L.M., Brannon, J.C., Podosek, F.A., 1990. New constraints on carbonate diagenesis from integrated Sr and S isotopic and rare earth element data, Jurassic Smackover Formation, U.S. *Gulf Coast. Appl. Geochemistry* 5, 449–470.
- Musgrove, M., Stern, L.A., Banner, J.L., 2010. Springwater geochemistry at Honey Creek State Natural Area, central Texas: Implications for surface water and groundwater interaction in a karst aquifer. *J. Hydrol.* 388, 144–156. <https://doi.org/10.1016/j.jhydrol.2010.04.036>
- Musgrove, M.L., Banner, J.L., 2004. Controls on the spatial and temporal variability of vadose dripwater geochemistry: Edwards aquifer, central Texas. *Geochim. Cosmochim. Acta* 68, 1007–1020. <https://doi.org/10.1016/j.gca.2003.08.014>

- Oetting, G.C., Banner, J.L., Sharp, J.M., 1996. Regional controls on the geochemical evolution of saline groundwaters in the Edwards aquifer, central Texas. *J. Hydrol.* 181, 251–283. [https://doi.org/10.1016/0022-1694\(95\)02906-0](https://doi.org/10.1016/0022-1694(95)02906-0)
- Ohr, M., Halliday, A.N., Peacor, D.R., 1991. Sr and Nd isotopic evidence for punctuated clay diagenesis, Texas Gulf Coast. *Earth Planet. Sci. Lett.* 105, 110–126. [https://doi.org/10.1016/0012-821X\(91\)90124-Z](https://doi.org/10.1016/0012-821X(91)90124-Z)
- Otero, C.L., Petri, B.L., 2010. Quality of Groundwater at and near an Aquifer Storage and Recovery Site, Bexar, Atascosa, and Wilson Counties, Texas, June 2004–August 2008.
- Paine, R.T., 1969. A Note on Trophic Complexity and Community Stability. *Am. Nat.* 103, 91–93. <https://doi.org/10.1086/282586>
- Pettorelli, N., Vik, J.O., Mysterud, A., Gaillard, J.M., Tucker, C.J., Stenseth, N.C., 2005. Using the satellite-derived NDVI to assess ecological responses to environmental change. *Trends Ecol. Evol.* 20, 503–510. <https://doi.org/10.1016/j.tree.2005.05.011>
- Pinter, N., Fiedel, S., Keeley, J.E., 2011. Fire and vegetation shifts in the Americas at the vanguard of Paleoindian migration. *Quat. Sci. Rev.* 30, 269–272. <https://doi.org/10.1016/j.quascirev.2010.12.010>
- Posey, H.H., Kyle, J.R., Jackson, T.J., Hurst, S.D., Price, P.E., 1987. Multiple fluid components of salt diapirs and salt dome cap rocks, Gulf Coast, U.S.A. *Appl. Geochemistry* 1 2, 523–534.
- Price, T.D., Connor, M., Parsen, J.D., 1985. Bone chemistry and the reconstruction of diet: Strontium discrimination in white-tailed deer. *J. Archaeol. Sci.* 12, 419–442.
- Samuelsen, J., 2020. An Isotopic Assessment of Late Prehistoric Interregional Warfare in the Southcentral US.
- Samuelsen, J.R., Potra, A., 2020. Biologically available Pb: A method for ancient human sourcing using Pb isotopes from prehistoric animal tooth enamel. *J. Archaeol. Sci.* 115, 105079. <https://doi.org/10.1016/j.jas.2020.105079>
- Sawyer, H., Middleton, A.D., Hayes, M.M., Kauffman, M.J., Monteith, K.L., 2016. The extra mile: Ungulate migration distance alters the use of seasonal range and exposure to anthropogenic risk. *Ecosphere* 7, 1–11. <https://doi.org/10.1002/ecs2.1534>
- Sellers, P.J., Berry, J.A., Collatz, G.J., Field, C.B., Hall, F.G., 1992. Canopy reflectance, photosynthesis, and transpiration. III. A reanalysis using improved leaf models and a new canopy integration scheme. *Remote Sens. Environ.* 42, 187–216. [https://doi.org/10.1016/0034-4257\(92\)90102-P](https://doi.org/10.1016/0034-4257(92)90102-P)
- Singh, R.R., Goyal, S.P., Khanna, P.P., Mukherjee, P.K., Sukumar, R., 2006. Using

- morphometric and analytical techniques to characterize elephant ivory. *Forensic Sci. Int.* 162, 144–151. <https://doi.org/10.1016/j.forsciint.2006.06.028>
- Smith Enos, J., Kyle, J.R., 2002. Diagenesis of the Carrizo Sandstone at Butler Salt Dome, East Texas basin, U.S.A.: Evidence for fluid-sediment interaction near halokinetic structures. *J. Sediment. Res.* 72, 68–81. <https://doi.org/10.1306/061101720068>
- Smith, F.A., Elliott Smith, R.E., Lyons, S.K., Payne, J.L., Villaseñor, A., 2019. The accelerating influence of humans on mammalian macroecological patterns over the late Quaternary. *Quat. Sci. Rev.* 211, 1–16. <https://doi.org/10.1016/j.quascirev.2019.02.031>
- Solis, K., 2020. An analysis of hunter-gatherer territoriality and post-marital residence patterns in the late archaic Texas coastal plain using strontium radiogenic isotopes ($^{87}\text{Sr}/^{86}\text{Sr}$).
- Szép, T., Møller, A.P., Piper, S., Nuttall, R., Szabó, Z.D., Pap, P.L., 2006. Searching for potential wintering and migration areas of a Danish Barn Swallow population in South Africa by correlating NDVI with survival estimates. *J. Ornithol.* 147, 245–253. <https://doi.org/10.1007/s10336-006-0060-x>
- Thompson, J.C., Wright, D.K., Ivory, S.J., 2021. The emergence and intensification of early hunter-gatherer niche construction. *Evol. Anthropol.* 30, 17–27. <https://doi.org/10.1002/evan.21877>
- Van Der Graaf, S., Stahl, J., Klimkowska, A., Bakker, J.P., Drent, R.H., 2006. Surfing on a green wave - How plant growth drives spring migration in the Barnacle Goose *Branta leucopsis*. *Ardea* 94, 567–577.
- Van Der Merwe, N.J., Lee-Thorp, J.A., Thackeray, J.F., Hall-Martin, A., Kruger, F.J., Coetzee, H., Bell, R.H.V., Lindeque, M., 1990. Source-area determination of elephant ivory by isotopic analysis. *Nature* 346, 744–746. <https://doi.org/10.1038/346744a0>
- Vereshchagin, N.K., Baryshnikov, G.F., 1991. The ecological structure of the “mammoth fauna” in Eurasia.” *Ann. Zool. Fennici* 28, 253–259.
- Wall, J., Wittemyer, G., Klinkenberg, B., LeMay, V., Douglas-Hamilton, I., 2013. Characterizing properties and drivers of long distance movements by elephants (*Loxodonta africana*) in the Gourma, Mali. *Biol. Conserv.* 157, 60–68. <https://doi.org/10.1016/j.biocon.2012.07.019>
- Western, D., 1975. Water availability and its influence on the structure and dynamics of a savannah large mammal community. *Afr. J. Ecol.* 13, 265–286. <https://doi.org/10.1111/j.1365-2028.1975.tb00139.x>
- Western, D., Lindsay, W.K., 1984. Seasonal herd dynamics of a savanna elephant population. *Afr. J. Ecol.* 22, 229–244. <https://doi.org/10.1111/j.1365-2028.1984.tb00699.x>

- Widga, C., Hodgins, G., Kolis, K., Lengyel, S., Saunders, J., Walker, J.D., Wanamaker, A.D., 2021. Life histories and niche dynamics in late Quaternary proboscideans from midwestern North America. *Quat. Res. (United States)* 100, 224–239. <https://doi.org/10.1017/qua.2020.85>
- Wiggins, W.D., 1986. Geochemical Signatures in Carbonate Matrix and Their Relation to Deposition and Diagenesis, Pennsylvanian Marble Falls Limestone, Central Texas. *J. Sediment. Res.* 56, 771–783.
- Wilmshurst, J.F., Fryxell, J.M., Farm, B.P., Sinclair, A.R.E., Henschel, C.P., 1999. Spatial distribution of Serengeti wildebeest in relation to resources. *Can. J. Zool.* 77, 1223–1232. <https://doi.org/10.1139/z99-088>
- Wong, C.L., 2013. Delineating controls on hydrologic variability and water geochemistry in central Texas.
- Wooller, M.J., Bataille, C., Druckenmiller, P., Erickson, G.M., Groves, P., Haubstock, N., Howe, T., Irrgeher, J., Mann, D., Moon, K., Potter, B.A., Prohaska, T., Rasic, J., Reuther, J., Shapiro, B., Spaleta, K.J., Willis, A.D., 2021. Lifetime mobility of an Arctic woolly mammoth. *Science (80-.)*. 373, 806–808. <https://doi.org/10.1126/science.abg1134>

Figures and Tables

Figure 1: Animation of Normalized Difference Vegetation Index for the state of Texas between 1 Jan 2013 and 1 Jan 2014. The colors correspond to satellite imagery. As the green becomes darker, it is assumed that vegetation is more productive. This shift primarily occurs between April and August.

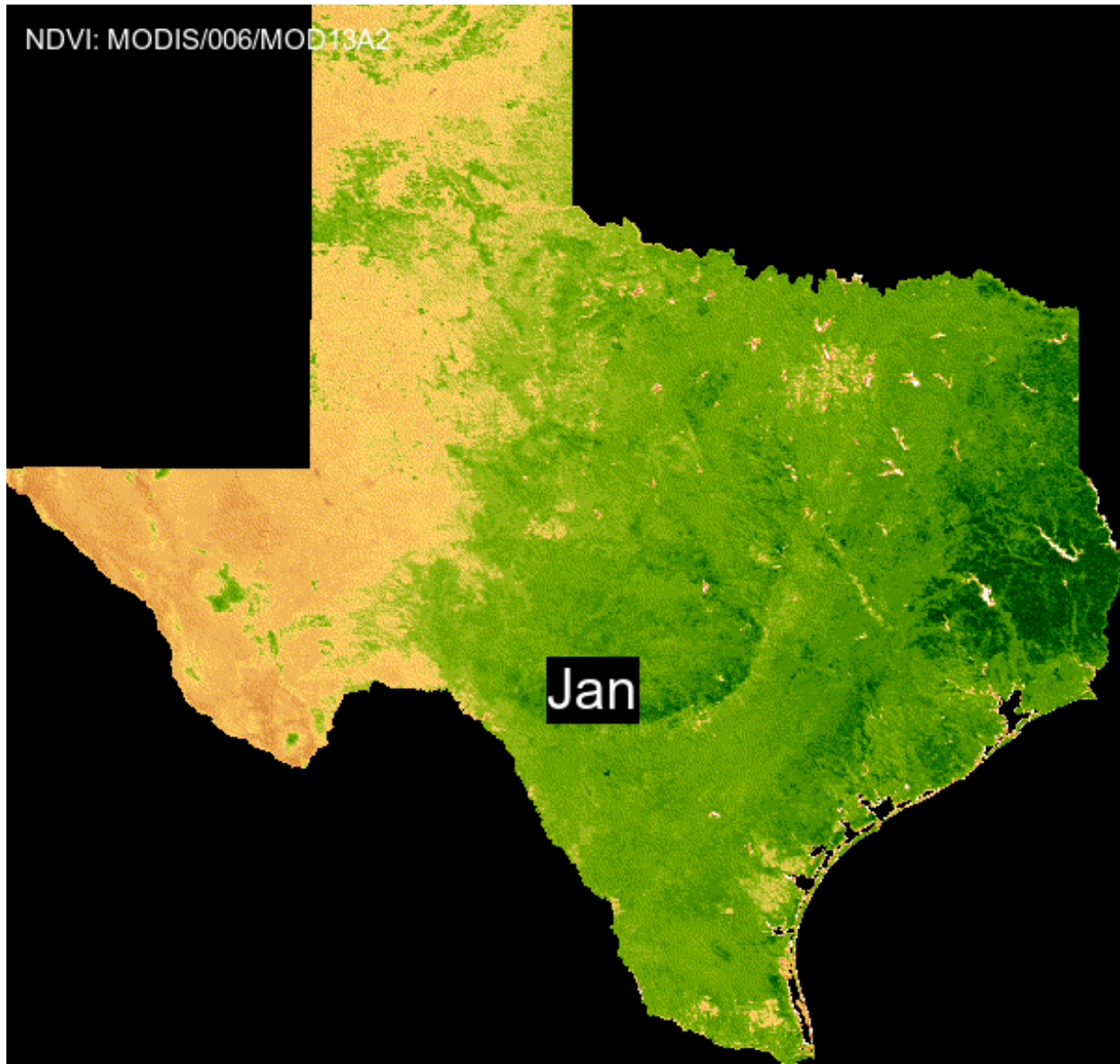


Figure 2: Map of the strontium variation across central and eastern Texas including all data points used in the new isoscape. The colors of the points corresponds to the substrate type, while the map follows a gradient from dark blue to dark red associated with low to high strontium ratios.

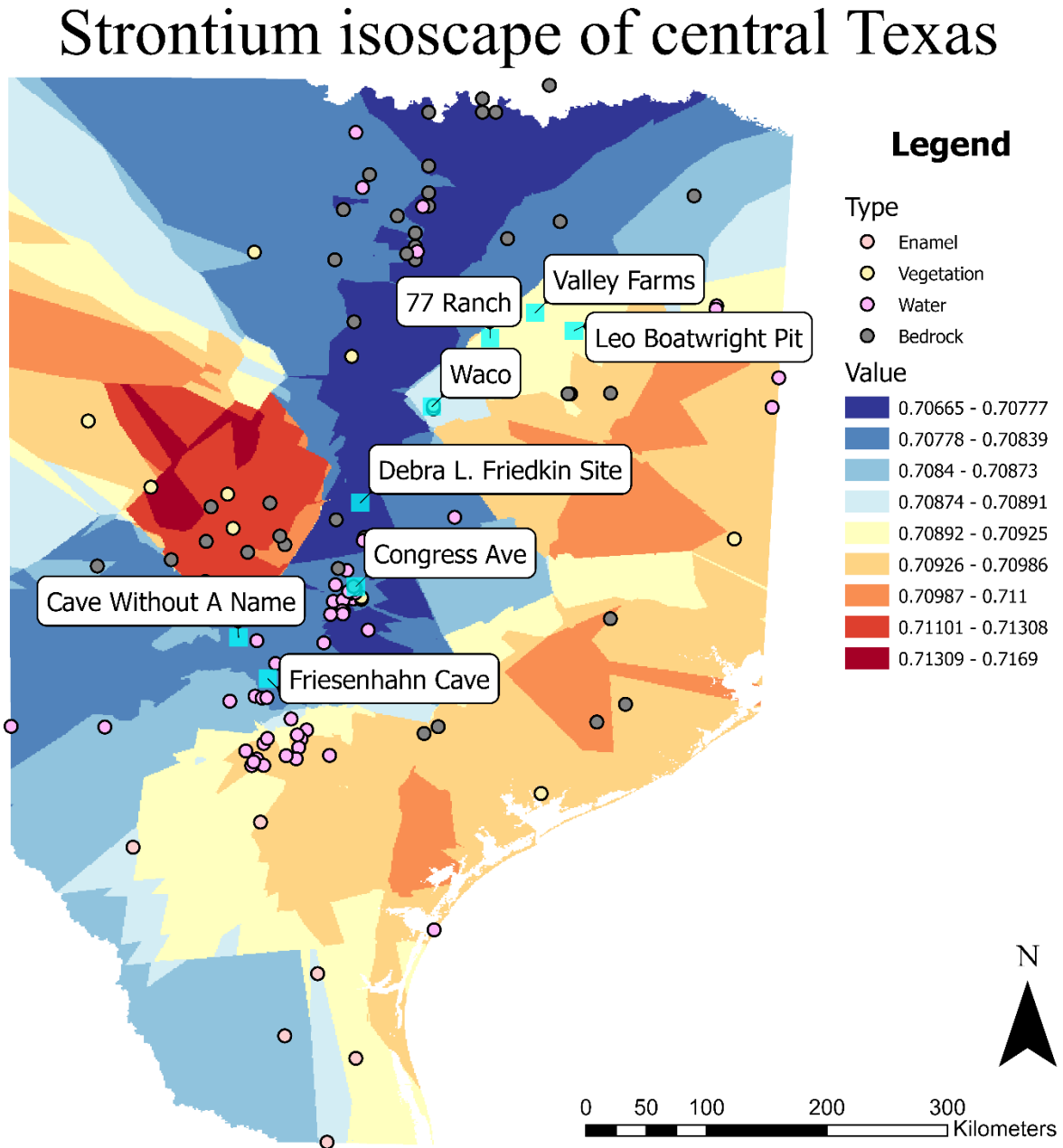


Figure 3: Map of all sites included in this study as well as the ecoregions and major rivers of Texas. Most sites (n=5) are located within the Blackland Prairie with Waco being in the Cross Timbers and Cave Without A Name in the the Edwards Plateau. Nearly all sites included in the study are located along a major river of Texas, except for 77 Ranch which is in between two major rivers of Texas.

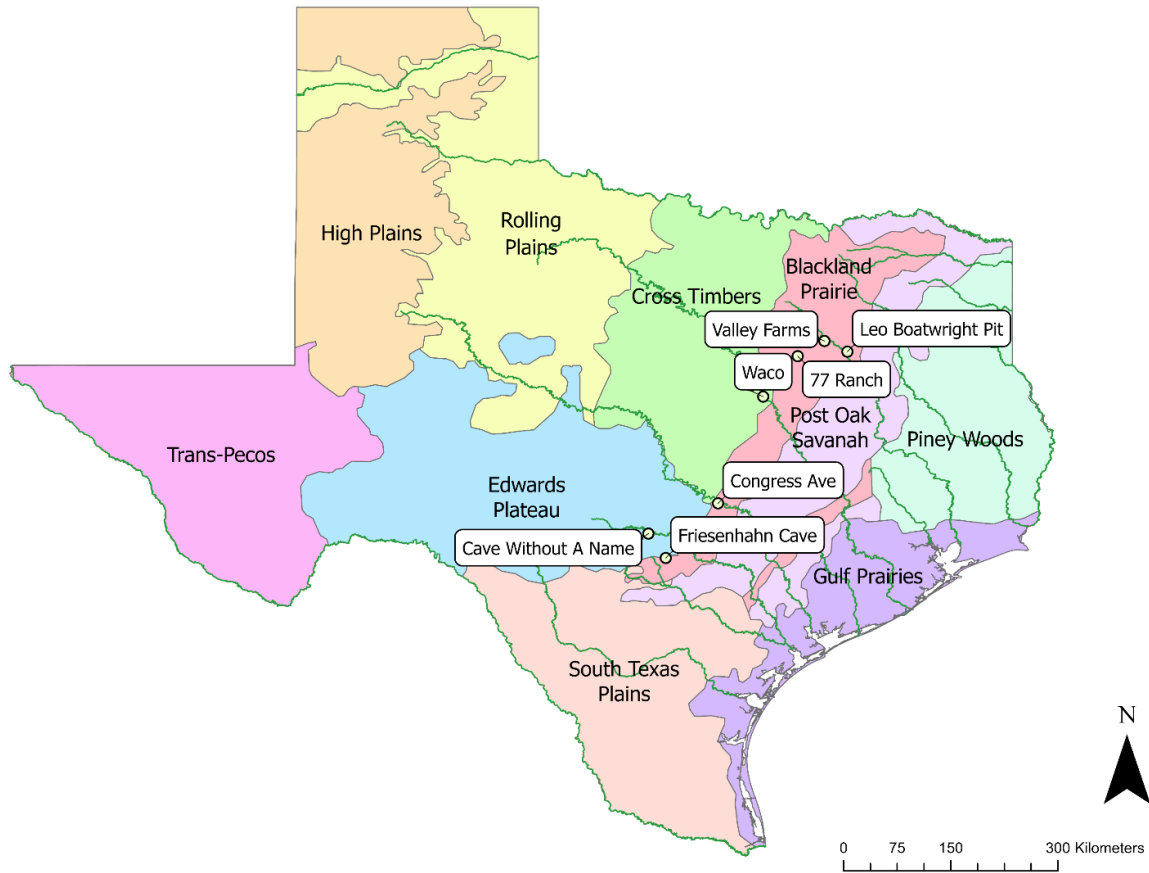


Figure 4: A strontium isoscape from multiple substrates – vegetation, enamel, water, and bedrock – for central Texas (n = 594). The color ramp goes from dark blue with the lower strontium ratios to dark red for the greater strontium ratios. Also included in this map is the Debra L. Friedkin Site, a proposed early human occupation site that temporally overlaps with Cave Without A Name and 77 Ranch.

Strontium isoscape of central Texas

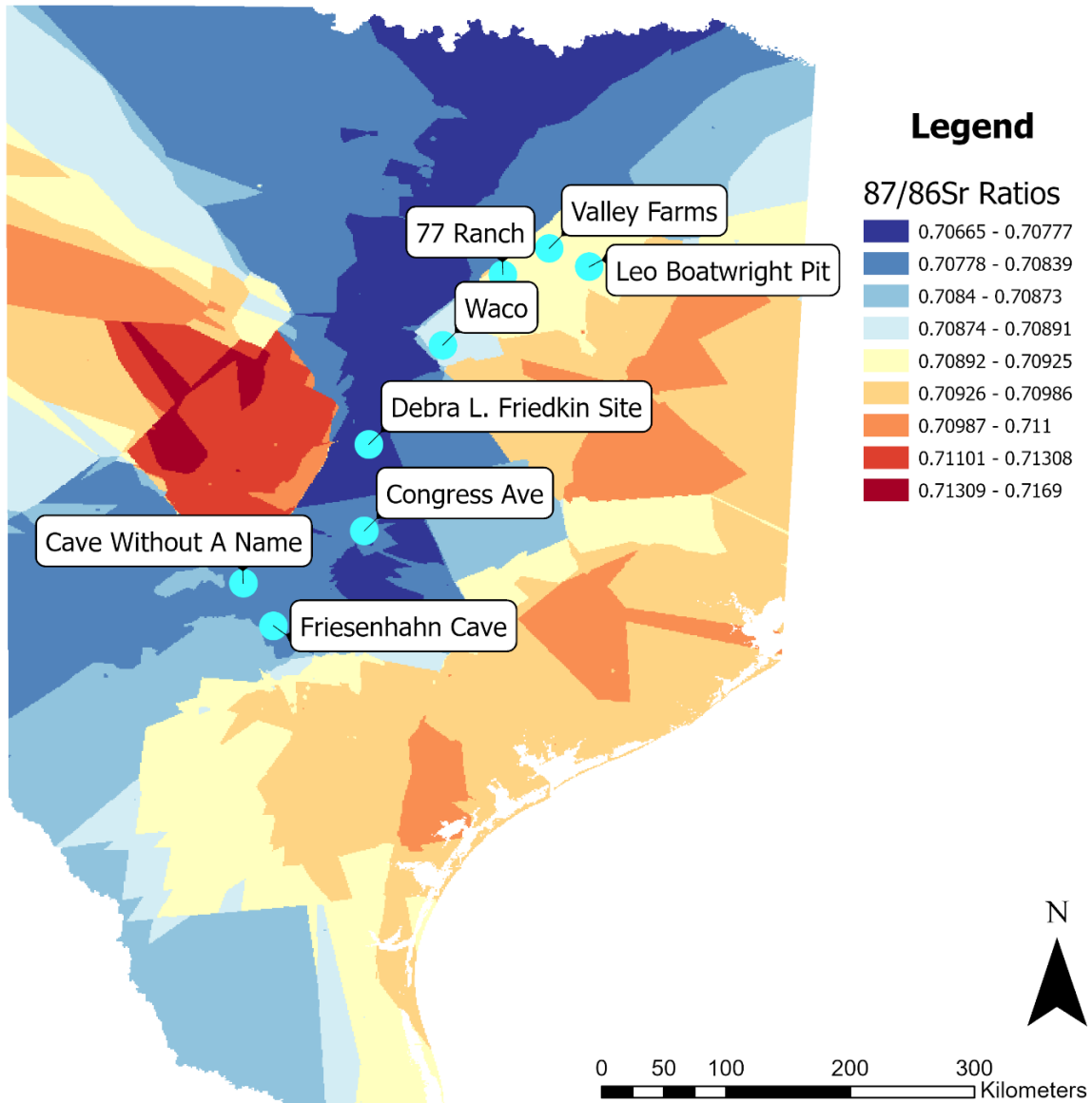


Figure 5: Strontium ratios for Pleistocene mammoths plotted from root to crown (i.e. youngest to oldest). The colors on this and the subsequent figures matches the color ramp for the isoscape to reflect the most likely areas for an individual to have spent the majority of their time at any given point. The red boxes represent the local strontium range within 50km of each site.

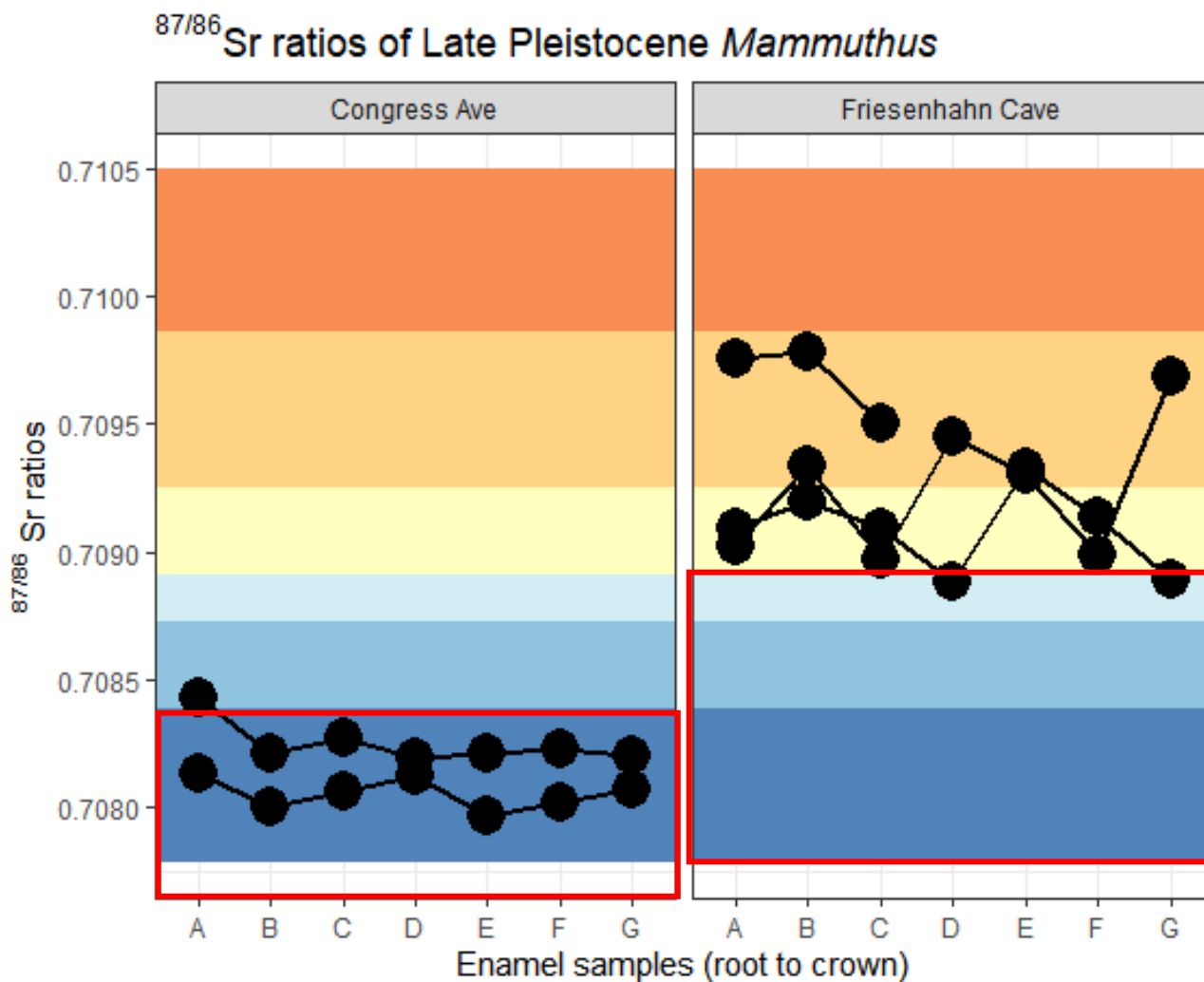


Figure 6: Strontium ratios for Pleistocene bison plotted from root to crown (i.e. youngest to oldest). The colors on this and the subsequent figures match the color ramp for the isoscape to reflect the most likely areas for an individual to have spent the majority of their time at any given point. The red boxes represent the local strontium range within 50km of each site.

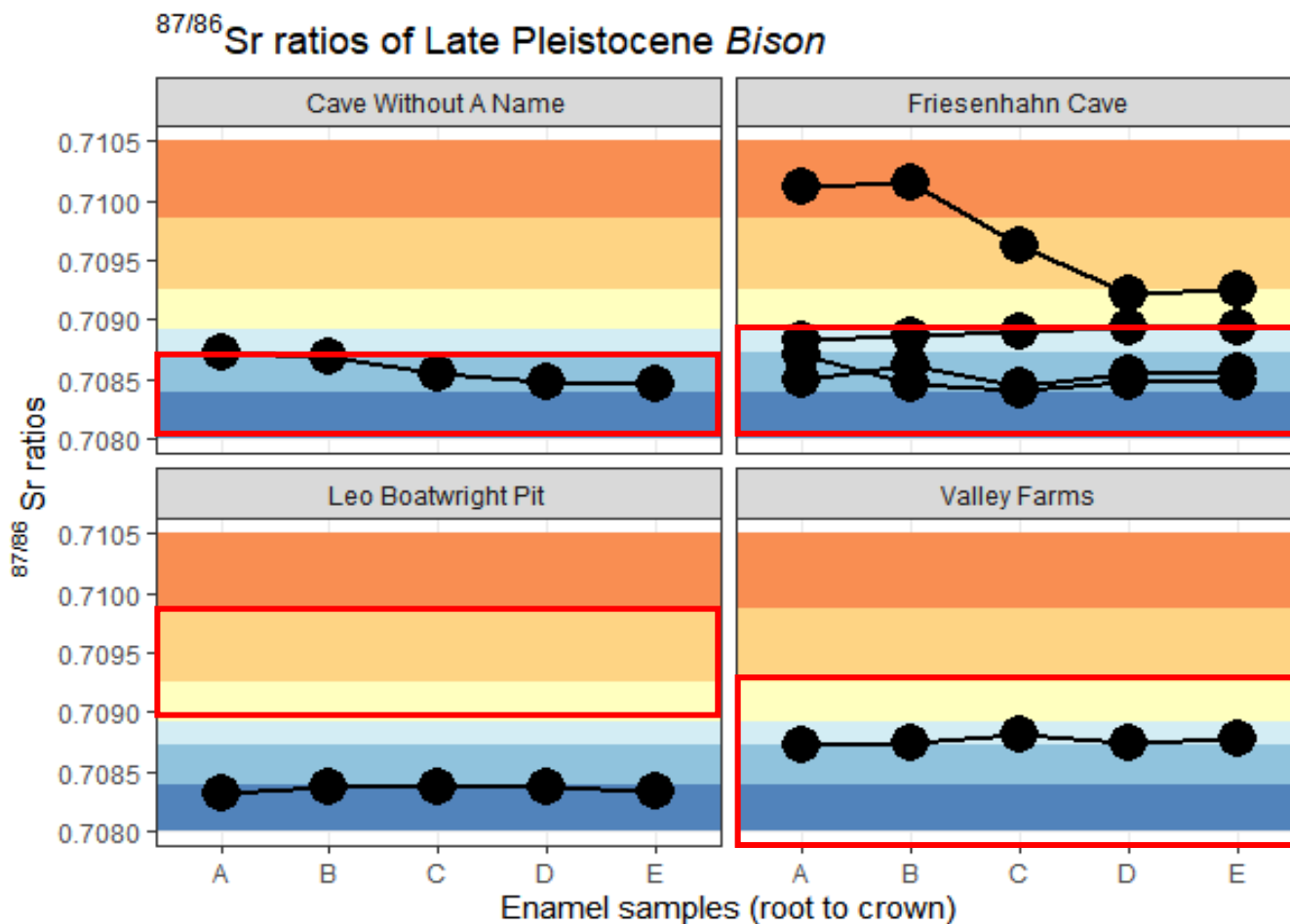


Figure 7: Strontium ratios for Holocene bison plotted from root to crown (i.e. youngest to oldest). The colors on this and the subsequent figures matches the color ramp for the isoscape to reflect the most likely areas for an individual to have spent the majority of their time at any given point. The red boxes represent the local strontium range within 50km of each site.

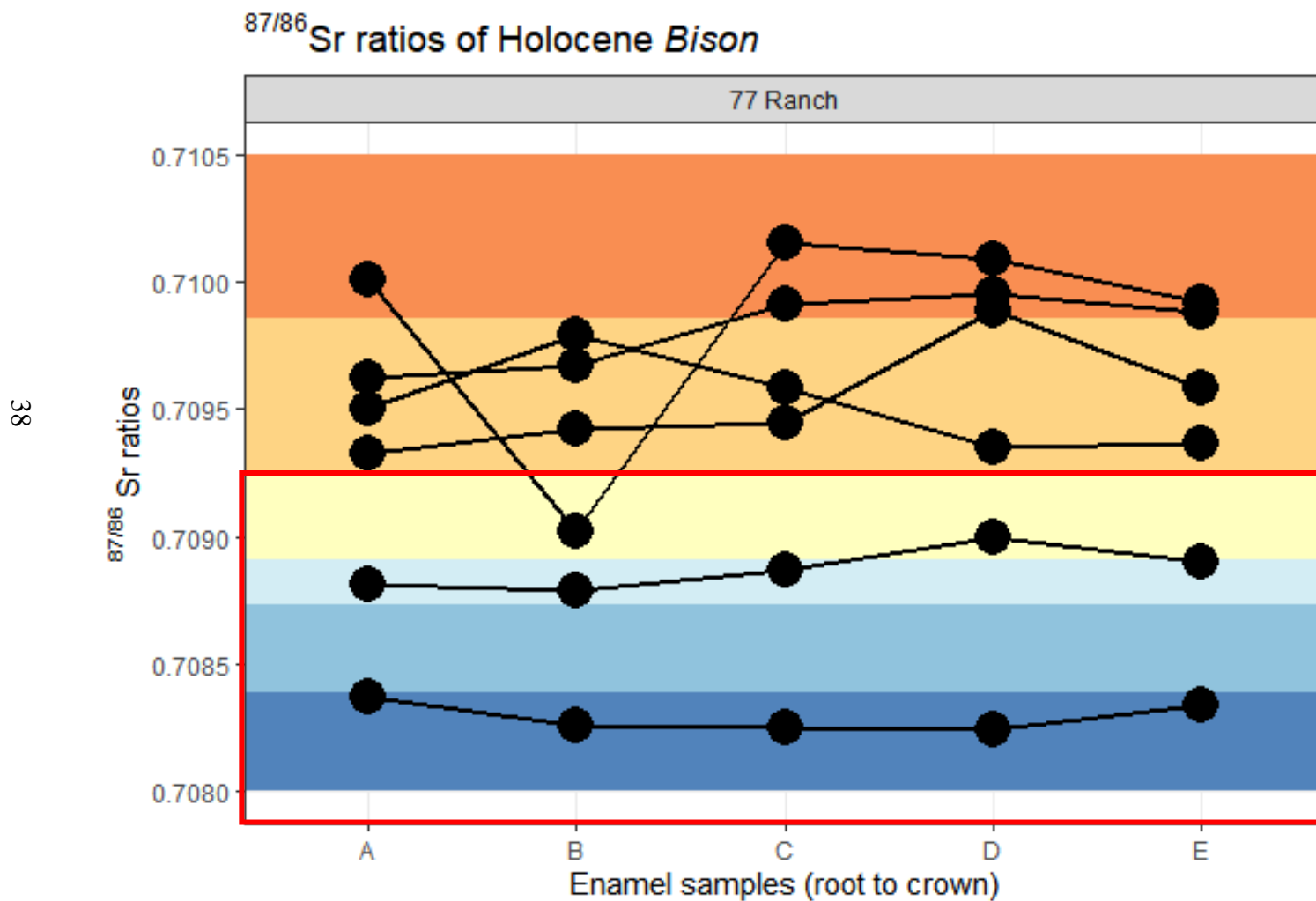


Figure 8: Strontium ratios for Friesenhahn Cave mammoths and bison plotted from root to crown (i.e. youngest to oldest). The colors on this and the subsequent figures matches the color ramp for the isoscape to reflect the most likely areas for an individual to have spent the majority of their time at any given point. The red boxes represent the local strontium range within 50km of each site.

39

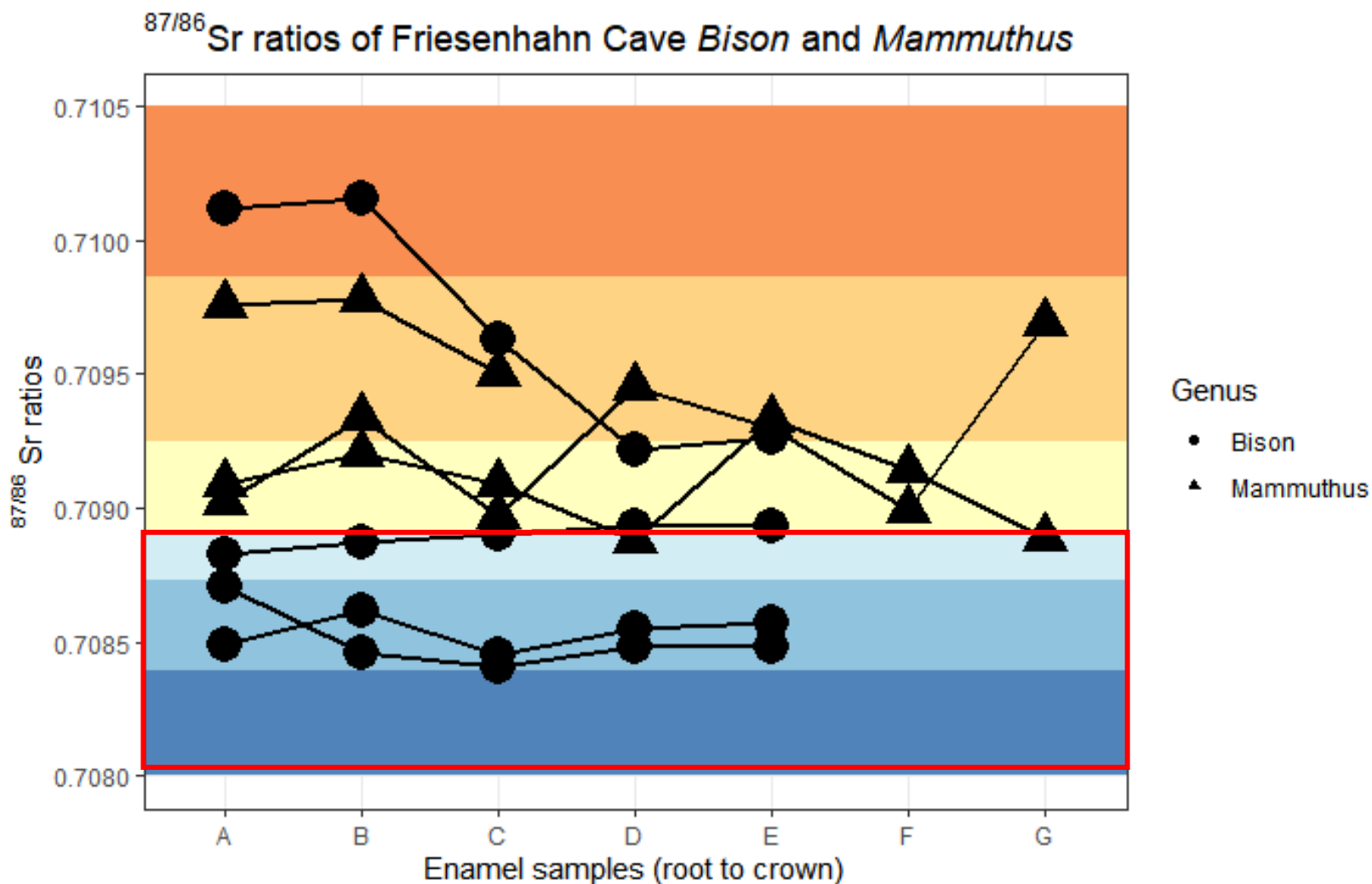
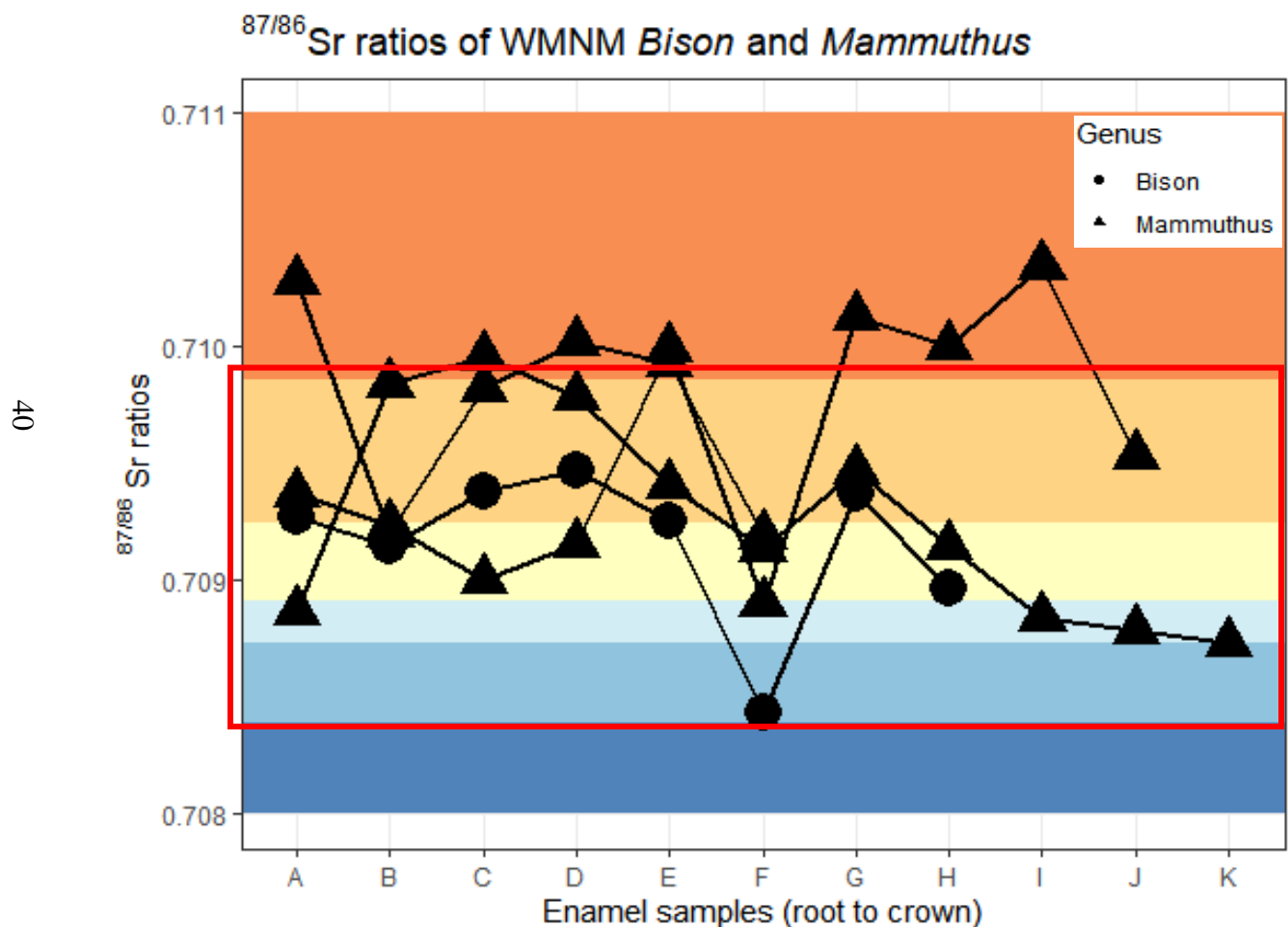


Figure 9: Strontium ratios for Waco Mammoth National Monument mammoths and bison plotted from root to crown (i.e. youngest to oldest). The colors on this and the subsequent figures matches the color ramp for the isoscape to reflect the most likely areas for an individual to have spent the majority of their time at any given point. The red boxes represent the local strontium range within 50km of each site.



40

Table 1: Table of ages, taxa, and sample sizes for each site included in this study arranged from oldest to youngest.

Site Name	Age	Taxa	N
Leo Boatright Pit	75 – 30 Ka ¹	Bison	1
Valley Farms	75 – 30 Ka ¹	Bison	1
Waco MNM	28 Ka ²	Mammoth	3
Waco MNM	28 Ka ²	Bison	1
Friesenhahn Cave	20 – 17.8 Ka ¹	Mammoth	3
Friesenhahn Cave	20 – 17.8 Ka ¹	Bison	4
Congress Avenue	19 – 15 Ka ¹	Mammoth	2
Cave Without A Name	11 Ka ¹	Bison	1
77 Ranch	Early Holocene ³	Bison	6

¹ Koch et al., 2004

² Esker et al., 2019

³ Clark Wernecke, personal communication

Table 2: Table of Esker and alternative maximum mixing model for Pleistocene mammoths. Percent X1 represent the estimated percent of time spent in the Smithson Paleosol, which underlies the Blackland Prairie and part of the Cross Timbers.

Specimen ID	Sample	Site Name	Percent X1 (Esker)	Percent X1 (Maximum)
1505	A	Friesenhahn Cave	47	78
	B		72	88
	C		61	84
	D		55	82
	E		73	89
	F		59	83
	G		71	88
2014	A	Friesenhahn Cave	75	90
	B		66	86
	C		60	83
	D		76	90
	E		68	87
	F		64	85
	G		68	85
2015	A	Friesenhahn Cave	54	81
	B		44	77
	C		44	77
37	A	Congress Ave	117	77

	B		119	74
	C		121	71
	D		115	79
	E		118	76
	F		120	73
	G		115	80
106	A	Congress Ave	112	84
	B		111	85
	C		112	84
	D		112	83
	E		109	88
	F		112	84
	G		103	96
72	A	Waco	72	89
	B		43	78
	C		39	77
	D		47	80
	E		82	89
	F		29	73
318	A	Waco	91	96
	B		89	96
	C		86	95

		D	74	90
		E	61	85
		F	74	90
		G	64	86
		H	49	80
		I	42	78
		J	47	79
		K	85	94
366	Waco	A	59	84
		B	26	72
		C	40	77
		D	35	75
		E	84	94
		F	40	77
		G	74	90
		H	80	92
		I	71	89
		J	65	87

Table 3: Table of Esker and alternative minimum mixing model for Pleistocene bison. Percent X1 represent the estimated percent of time spent in the Smithson Paleosol, which underlies the Blackland Prairie and part of the Cross Timbers.

Specimen ID	Sample	Site Name	Percent X1 (Esker)	Percent X1 (Minimum)
13	A	Leo Boatright Pit	107	90
	B		105	93
	C		105	93
	D		105	93
	E		106	91
2	A	Valley Farms	91	112
	B		90	113
	C		88	117
	D		90	113
	E		89	115
1190	A	Waco	81	93
	B		65	87
	C		103	101
	D		70	88
	E		61	85
	F		65	86
	G		74	90
	H		69	88
2198	A	Friesenhahn Cave	82	92

	B		91	96
	C		93	97
	D		90	96
	E		90	96
3285	A	Friesenhahn Cave	31	72
	B		30	71
	C		49	79
	D		64	85
	E		62	84
3390	A	Friesenhahn Cave	78	91
	B		76	90
	C		75	90
	D		74	89
	E		74	89
3403	A	Friesenhahn Cave	90	96
	B		85	94
	C		91	96
	D		88	95
	E		87	95
UNK	A	Cave Without A Name	91	112
	B		93	110
	C		98	102

D

101

98

E

102

98

Table 4: Table of Esker and alternative minimum mixing model for Holocene bison. Percent X1 represent the estimated percent of time spent in the Smithson Paleosol, which underlies the Blackland Prairie and part of the Cross Timbers.

Specimen ID	Sample	Site Name	Percent X1 (Esker)	Percent X1 (Minimum)
92	A	77 Ranch	88	117
	B		88	116
	C		85	120
	D		80	127
	E		84	122
138	A	77 Ranch	67	145
	B		63	150
	C		62	151
	D		44	175
	E		57	158
154	A	77 Ranch	105	93
	B		110	87
	C		110	86
	D		110	86
	E		106	91
157	A	77 Ranch	60	154
	B		48	170
	C		57	158
	D		66	146

	E		65	147
158	A	77 Ranch	40	182
	B		79	128
	C		34	189
	D		36	186
	E		43	177
160	A	77 Ranch	55	161
	B		53	163
	C		44	176
	D		42	178
	E		45	174